Radio view of the Milky Way

- Spectrum
- Characteristic Features
- SgrA* & the Galactic Black Hole

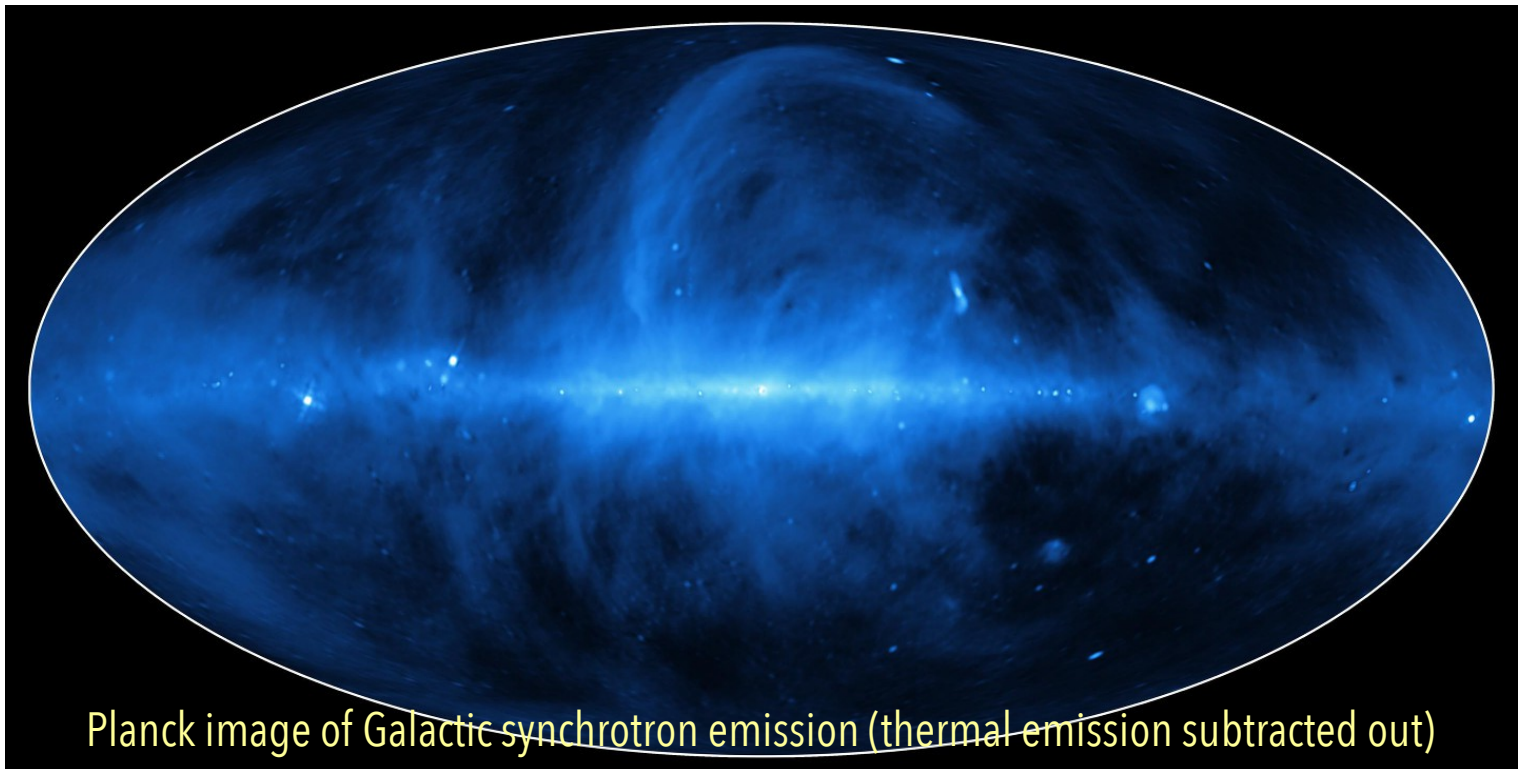

Planck image of Galactic synchrotron emission (thermal emission subtracted out)

The environment of the Milky Way in the radio band

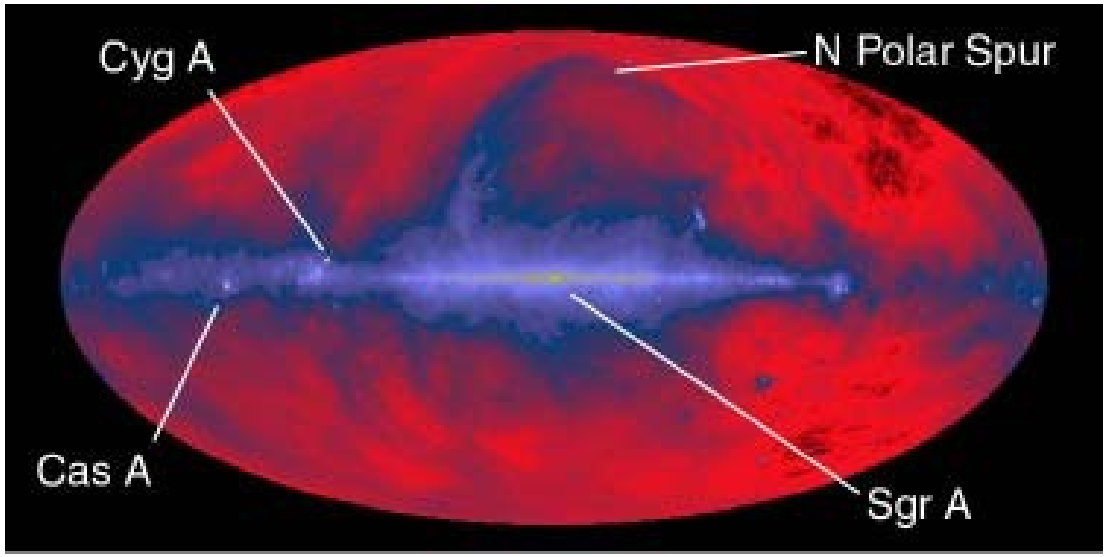

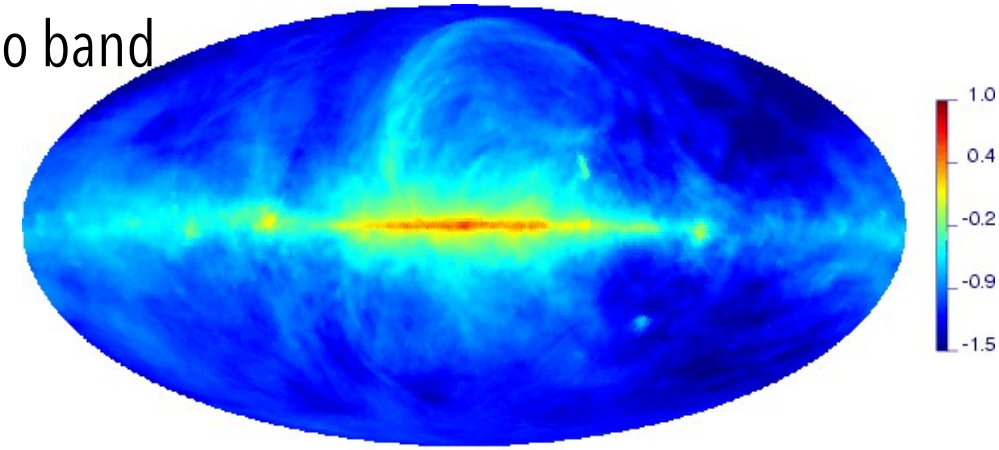

Model for Synchrotron emission

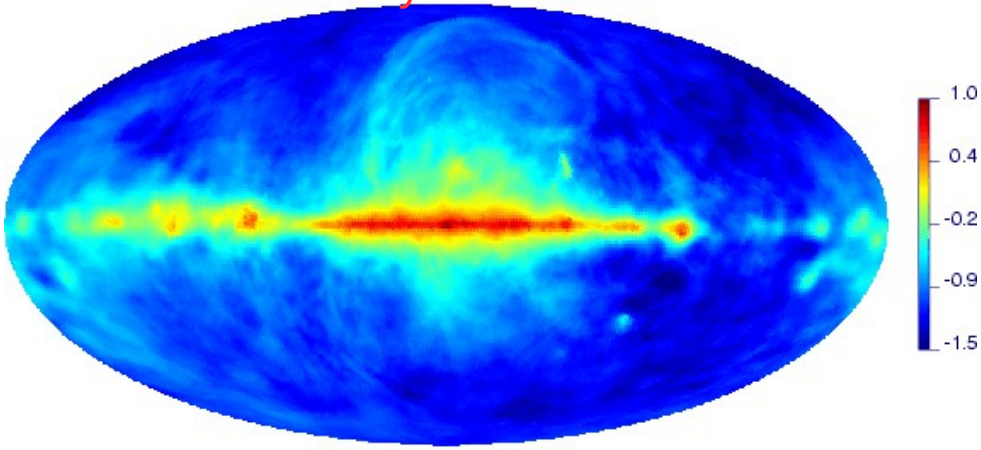

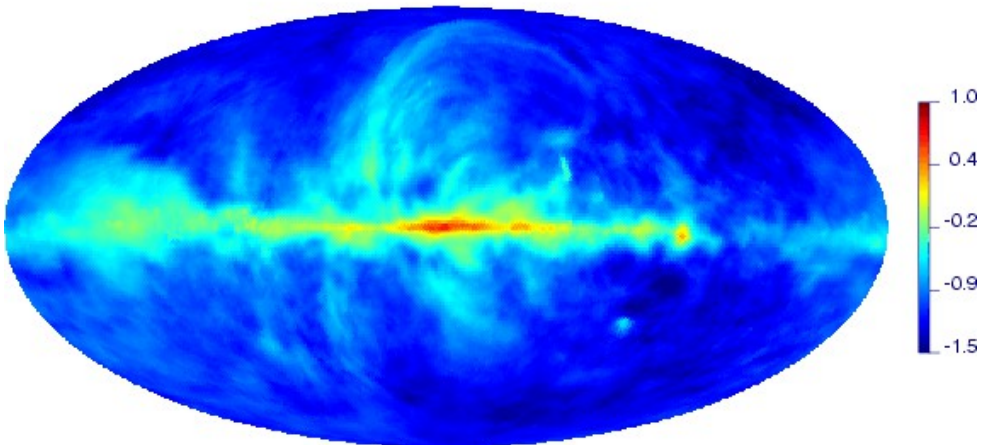

Bennett +, 2003

Multicolor WMAP images at various frequencies:

- Synchrotron is red,
- Free-free is green
- Thermal dust is blue.

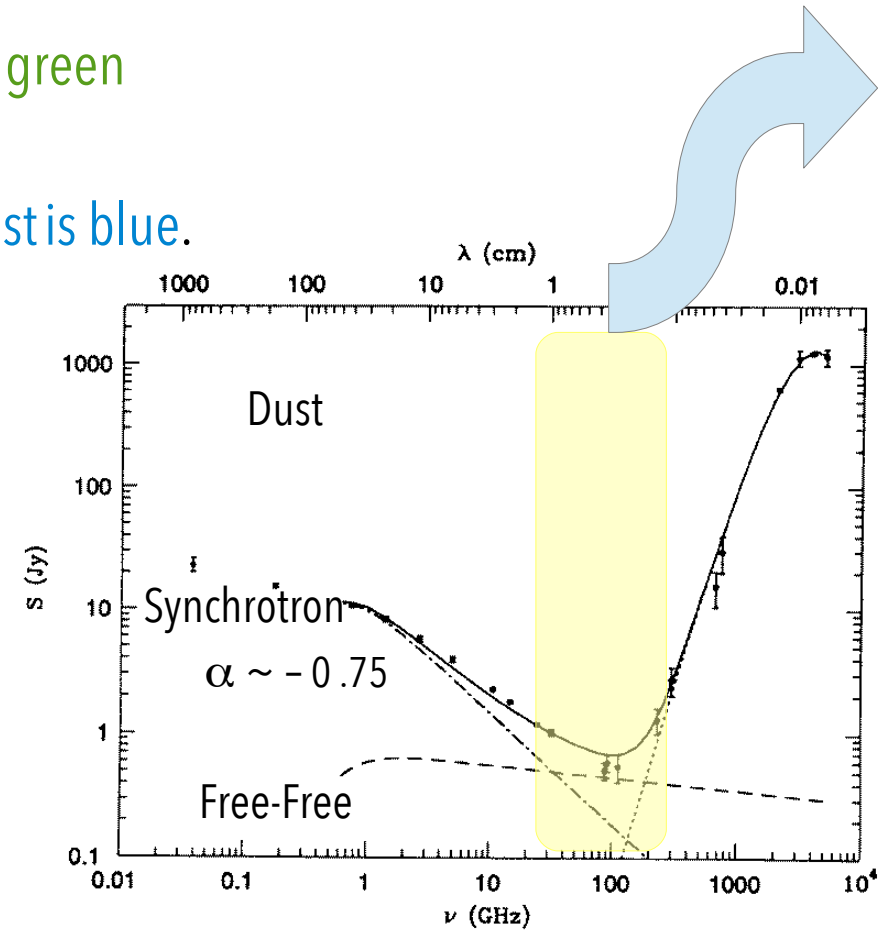

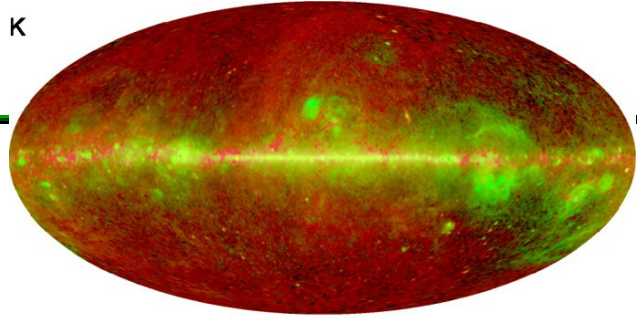

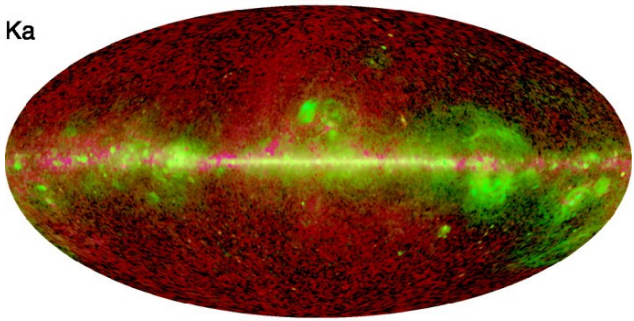

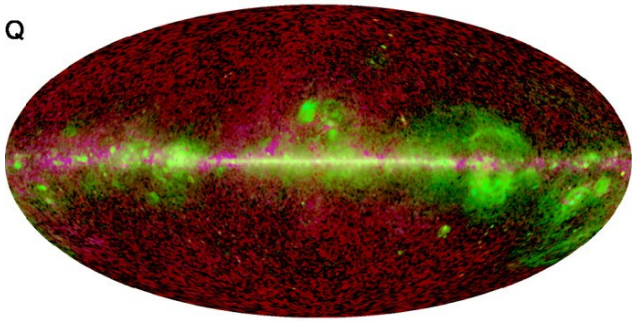

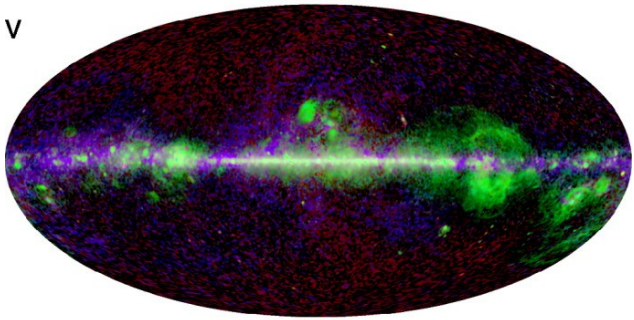

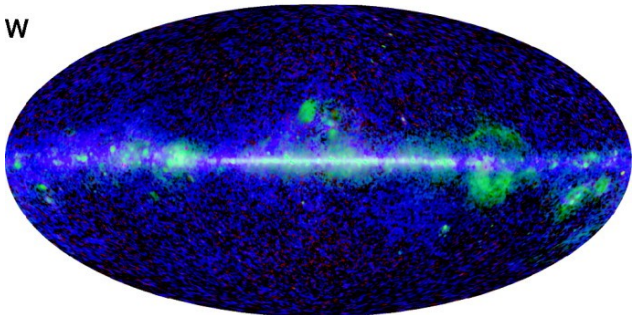

Electron energy spectral index distribution: Bennett +, 2003

Top (a) Haslam 408 MHz sky map, largely dominated by synchrotron emission.

Middle (b) 23 GHz *WMAP* map, also dominated by synchrotron emission, but more concentrated toward the plane. The steep spectral index North Galactic Spur, for example, is much less apparent at *WMAP* frequencies.

Bottom (c) Spectral index map of (408 MHz, 23 GHz) showing the flatter spectral index ($\delta \sim -2.5$) regions of active star formation in the plane, where the cosmic-ray electrons are generated. The steeper spectral index regions ($\delta \sim -3$) off the plane suggest the energy losses suffered by the cosmic-ray electrons during the period of time required for their diffusion away from the star formation regions of their origin. This spectral index map is dominated by synchrotron emission but still contains free-free emission.

It has been generated after setting zero points based on cosecant fits to both maps, which provides an absolute zero point for the *WMAP* map.

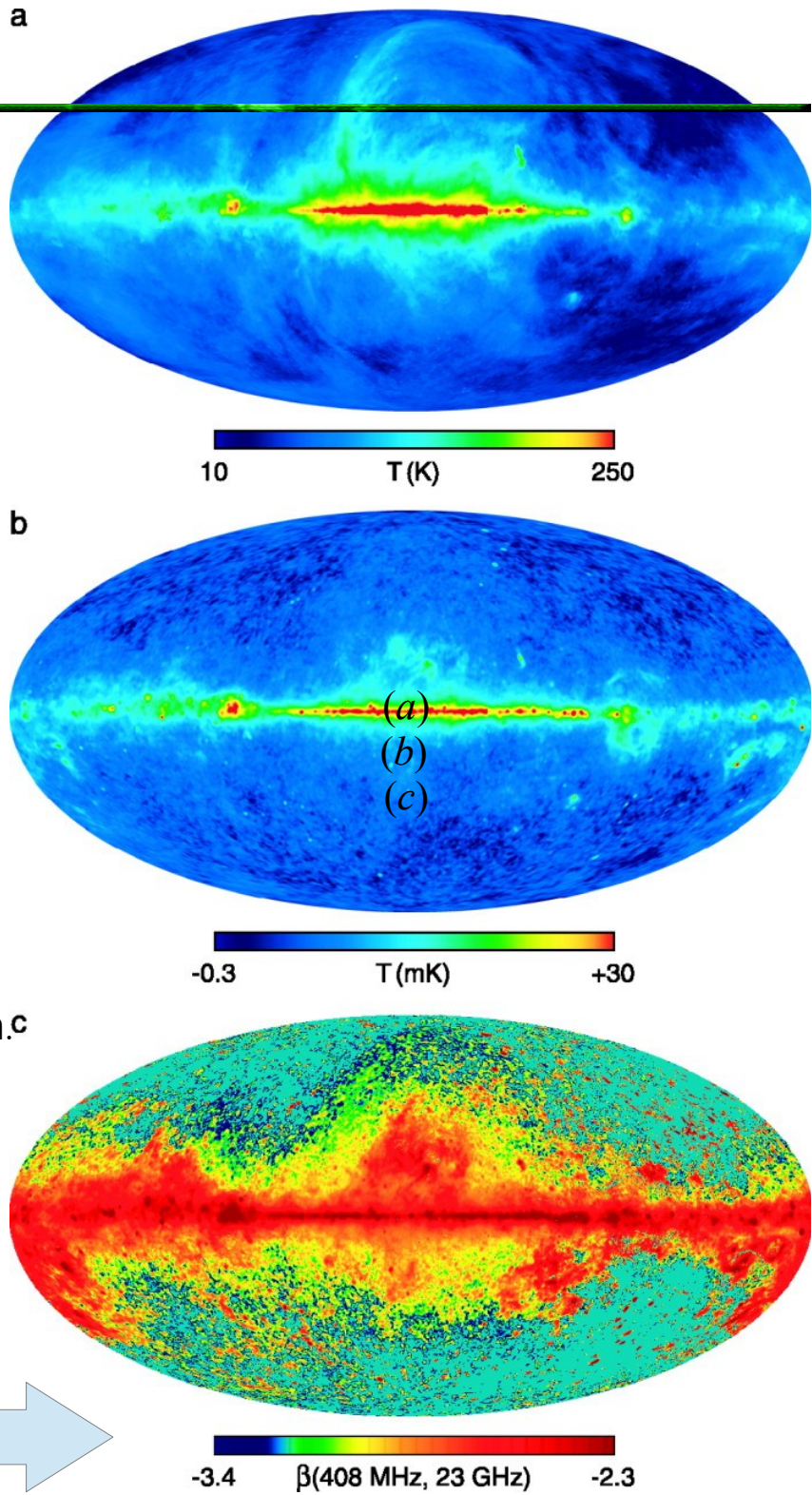

Electron energy spectral index distribution:
Miville-Deschênes +, 2008

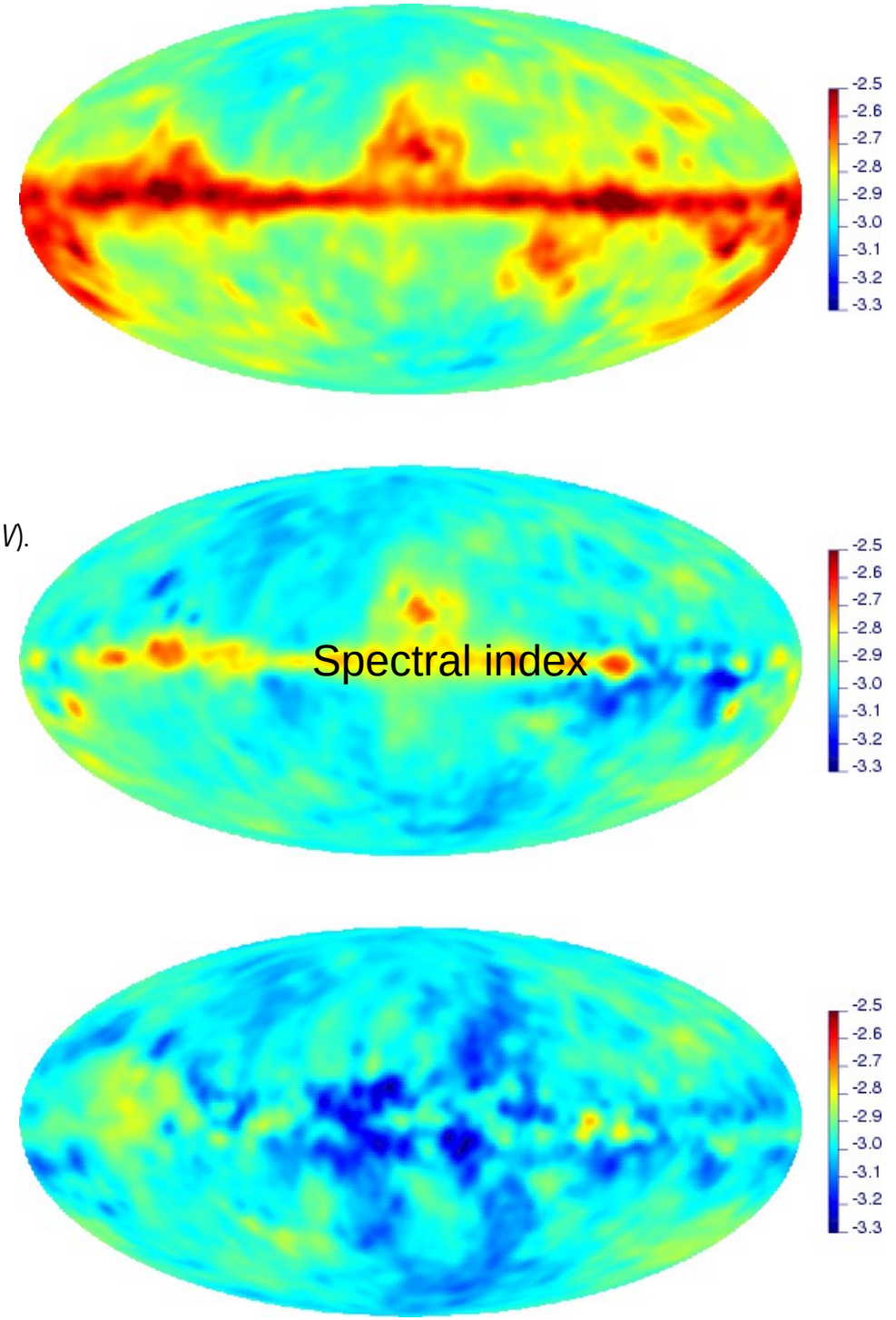

Figure 2: Synchrotron spectral index () between 408 MHz and 23 GHz.
All maps were smoothed at 5 deg .

Top: model 1 - this is making the assumption of no anomalous emission.
The map is similar to the one of (Bennett et al. 2003b, their Fig. 4).

Middle: model 3 - assumes a spinning dust component at 23 GHz which scales with *E*(*B*-*V*).

Bottom: model 4 - obtained from polarization data for MATH: $p=-8.5^\circ$,
MATH: $\chi_0=8^\circ$, MATH: $r_0=11^\circ$, and MATH:

$\sigma_{\rm turb}=1.7~\mu$ G.

The thermal emission, once a model for non-thermal has been subtracted

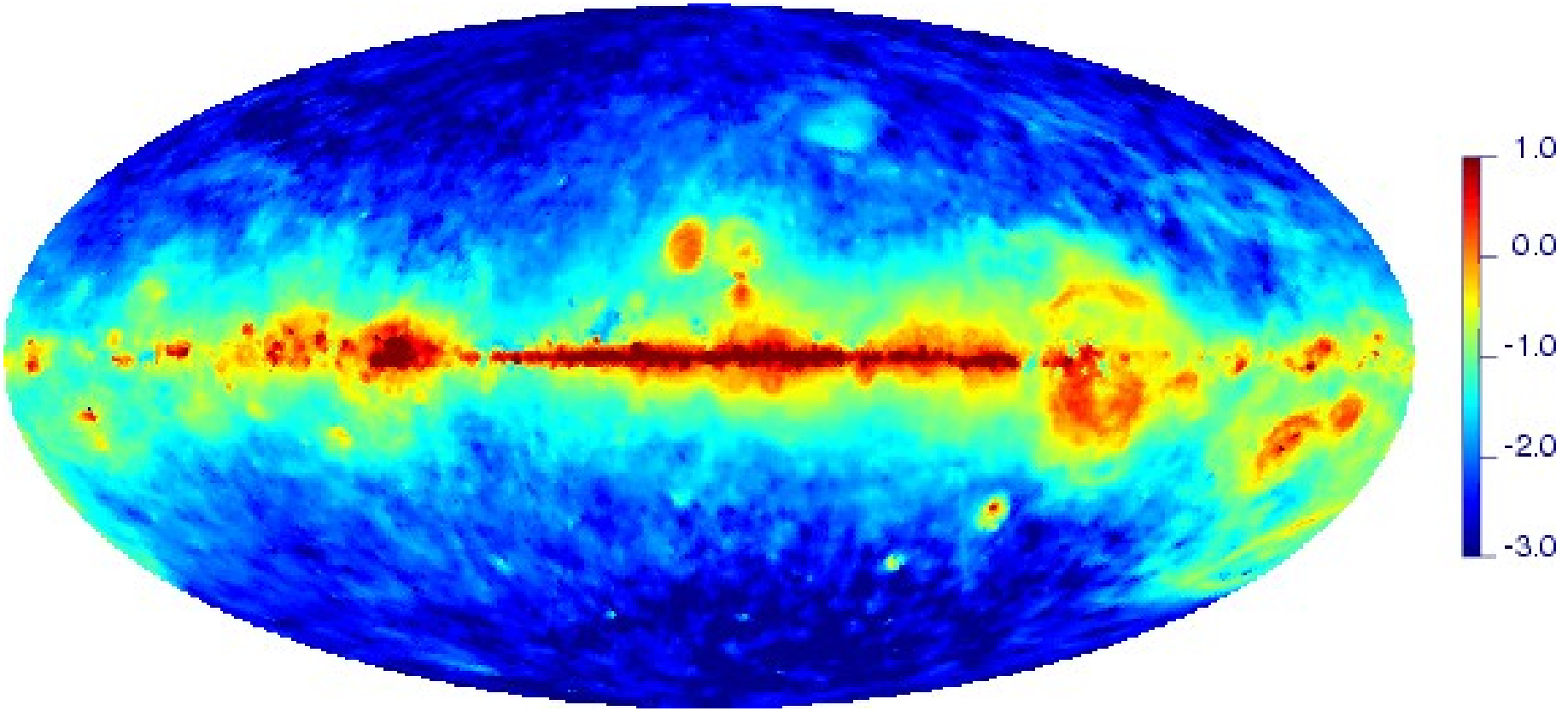

Free-Free emission at 23 GHz (in (mK)) estimated using H emission corrected for extinction (following Dickinson et al. 2003)
For E(B-V) > 2 , the free-free emission is the one obtained from the WMAP MEM decomposition.
For E(B-V) < 2, the free-free emissionis the one estimated using H emission, except when the WMAP MEM free-free is lower.

$$\mu \propto T^{-1/2}(1-e^{-h\nu/kT})\nu^{-3} \cong 0.018T^{-3/2}n_e n_z Z^2 \nu^{-2}\overline{g_{ff}}$$

Difficult to derive the total emission (resolution, additional contributions: thermal emission mostly $\pm 2^{\circ}$ within the disk)

$L_{Rtot} \approx 10^{38}$ erg

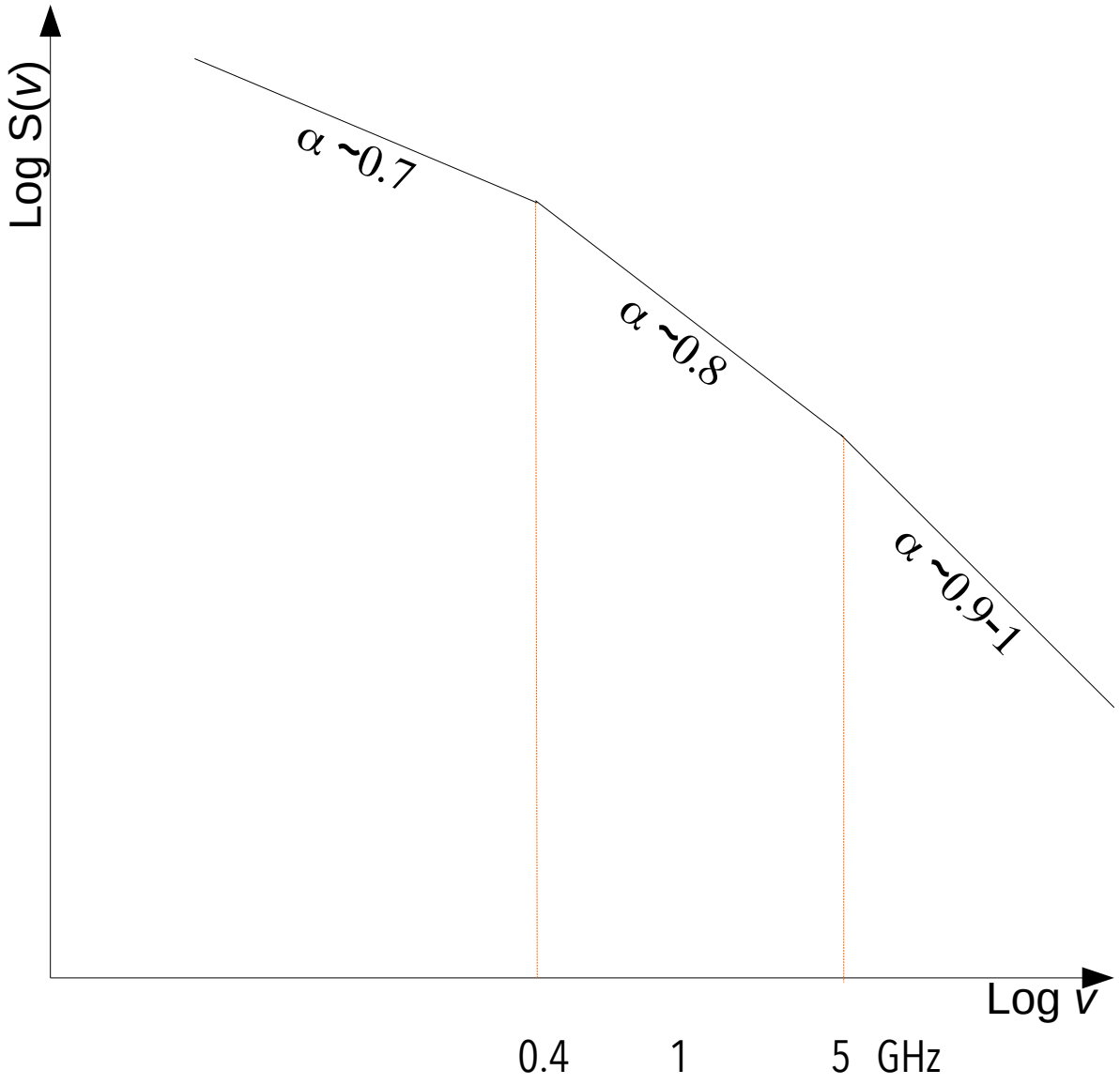

Historical measurements of δ [$N(E) = N_0 E^{-\delta}$]

Reference	Date	Freq.(MHz)	δ	Comments
Turtle	1962	100	2.5+/-0.1	
		176	2.9+/-0.1	
Andrew	1966	10-178	2.43+/-0.03	
Purton	1966	10-300	2.51+/-0.05	
Bridle	1967	81.5	2.38+/-0.03	Anticenter
		81.5	2.46+/-0.04	Inner arm
Webster	1974	408-610	2.80+/-0.05	Increases > 400 MHz
Sironi	1974	81.5-408	2.41+/-0.04	Average over regions out of plane
		151.5-408	2.49+/-0.04	
Rogers+	2008	100-200	2.5+/-0.1	
Bowman		150-408	2.52+/-0.04	

Parkes view of polarized emission

Linearly polarized intensity P at 2307 MHz from S-PASS. The thick dashed lines delineate the radio lobes, while the thin dashed lines delimit the gamma-ray Fermi Bubbles.

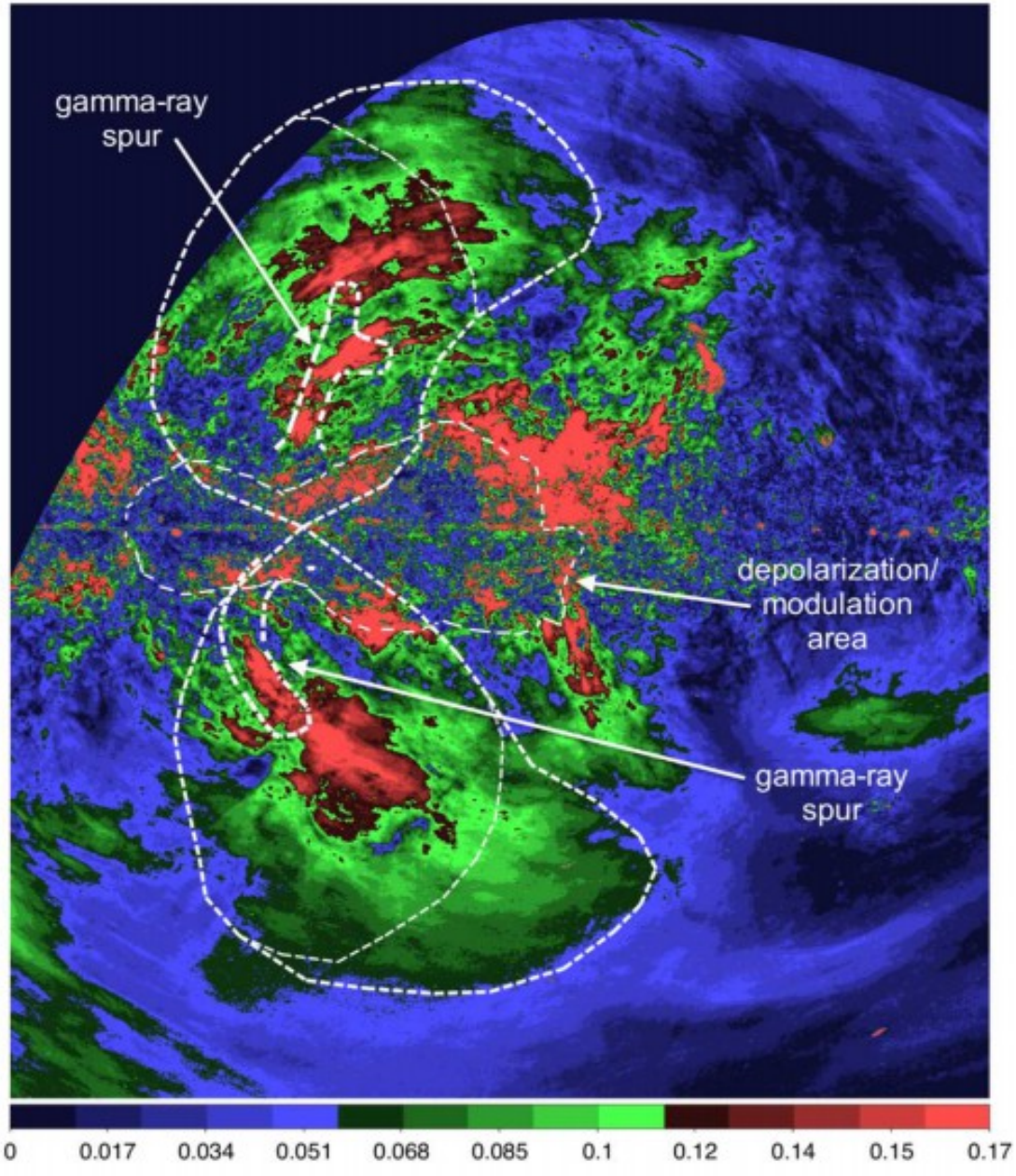

Carretti et al. 2013, Nature 493,66

Foot prints of the activity in the centre of the Milky Way:

Polarized intensity and magnetic angles at 23 GHz from WMAP. The radio lobes at 2.3 GHz are shown by the black solid lines. The magnetic field intensities are 6-12 μG for the lobes and 13-15 μG for the ridges.

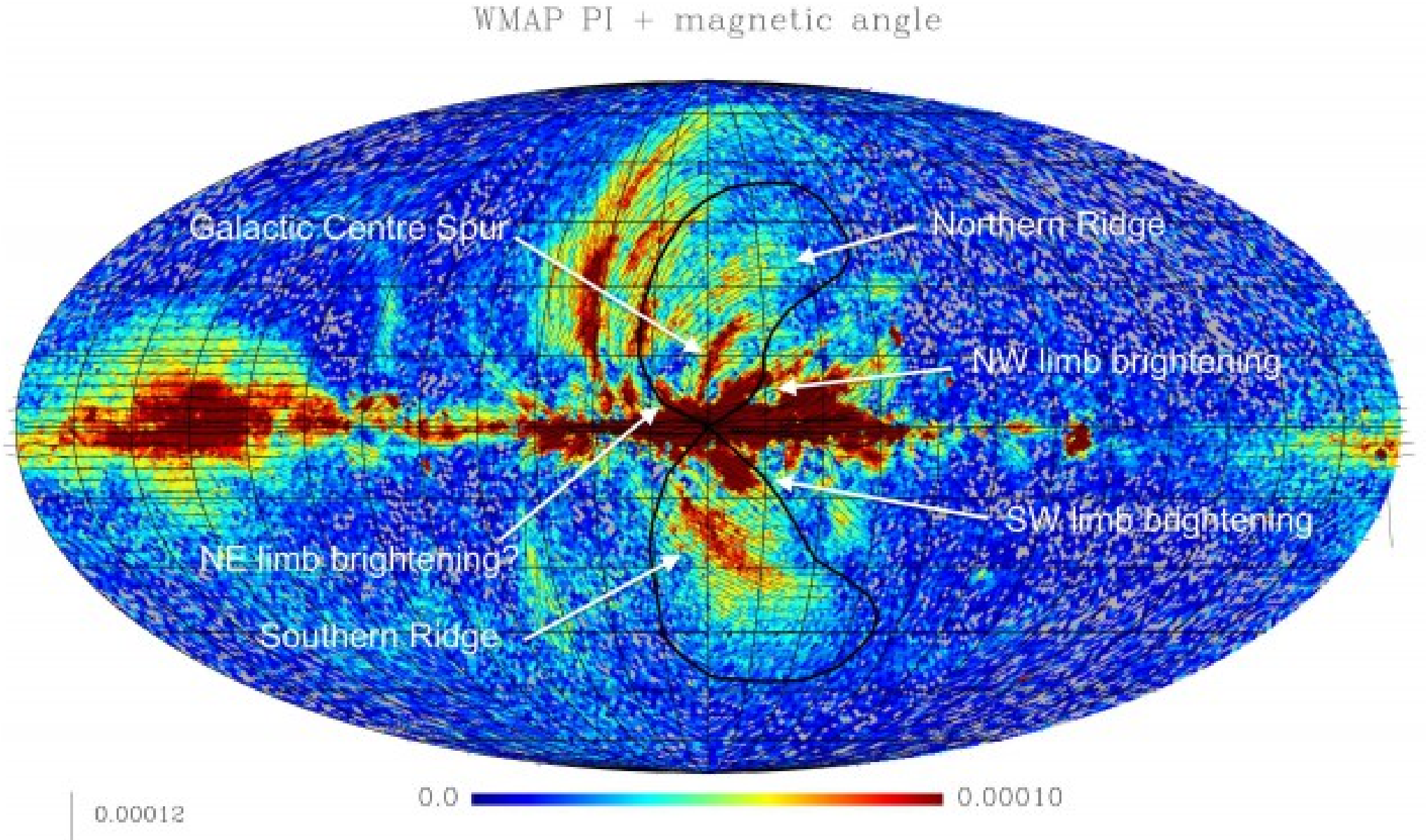

What else ?

- The spectral index (2.3-23.0 GHz) is ~ -1.0/-1.2 steepening with projected distance from the Galactic plane
- High polarization fraction(~ 25-31%) suggest that the lobes are due to cosmic-ray electrons, transported from the plane, synchrotron-radiating in a partly ordered magnetic field.
- The radio lobes originate in a biconical, star-formation driven (rather than black-hole-driven) outflow from the Galaxy's central 200 parsecs that transports a huge amount of magnetic energy, ~ 10^{55} ergs, into the Galactic halo.
- Let's search for the GC ...

Further reading: The Galactic Centre and Low Luminosity Black Holes

Melia & Falcke, 2001 , ARAA, 39, 309
" The Supermassive Black Hole at the Galactic Centre"

Morris & Serabyn, 1996, ARAA, 34, 645
"The Galactic Center Environment"

Yuan & Narayan, 2014, 52, 529
"Hot Accretion Flows Around Black Holes"

Yusef–Zadeh et al., ApJ., 808, 97
"Signatures of Young Star Formation Activity within Two Parsecs of SgrA*"

⇒ A weak "core" is often found in all (spiral galaxies) galaxies.

Fox et al. 2015

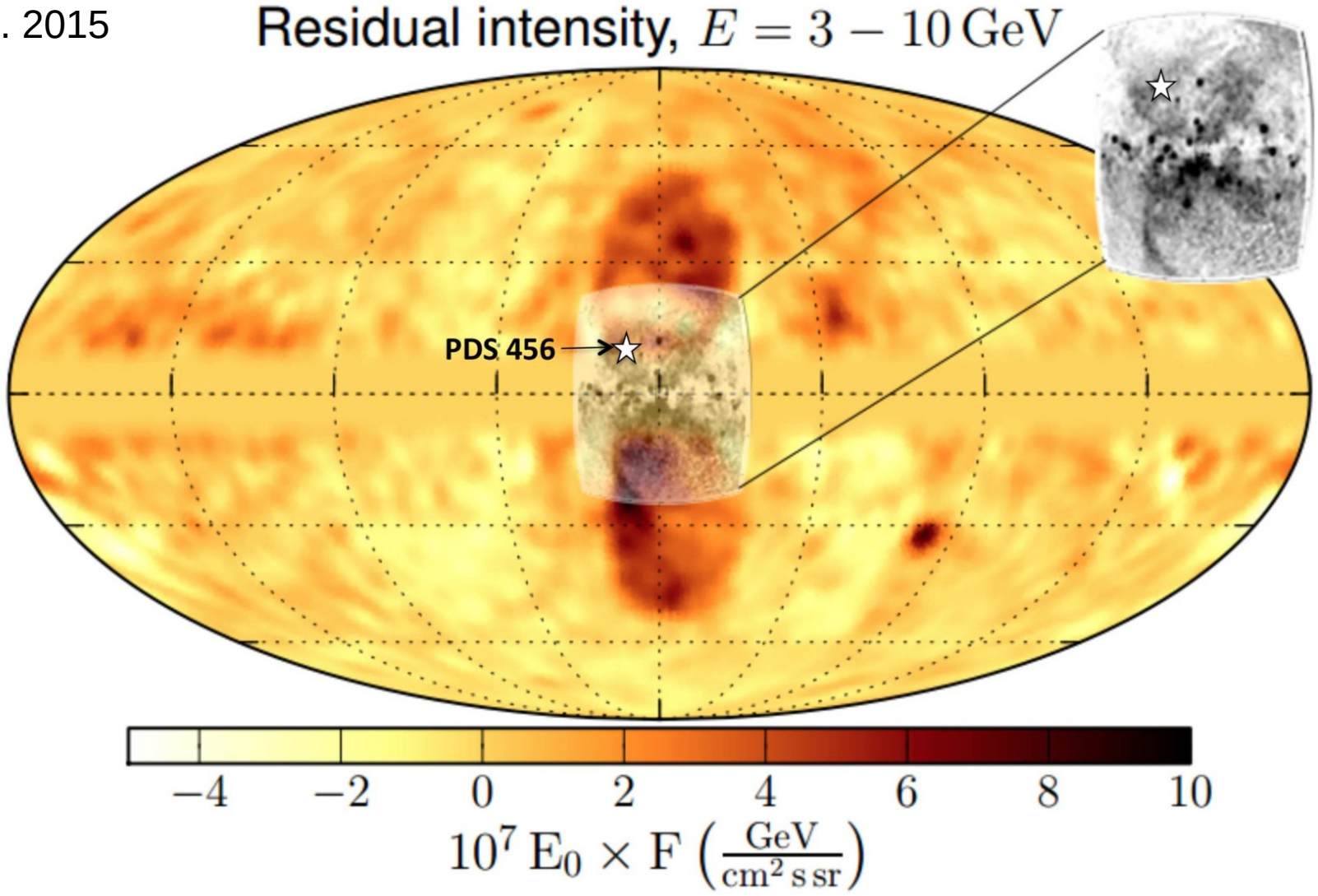

FIG. 1.— Collage of gamma-ray and X-ray emission showing the striking biconical nuclear structure intercepted by the PDS 456 sightline. The yellow/orange map is an all-sky *Fermi* image of the residual gamma-ray intensity in the 3–10 GeV range, in Galactic coordinates centered on the GC (Ackermann et al. 2014; © AAS. Reproduced with permission). The Fermi Bubbles are the twin lobes in dark orange at the center of the figure. Superimposed in gray-scale is the *ROSAT* diffuse 1.5 keV emission map, based on Snowden et al. 1997, Bland-Hawthorn & Cohen 2003, and Veilleux et al. 2005. The inset on the right shows a zoom-in on the X-ray data. Adapted from Figure 22, *The Spectrum and Morphology of the Fermi Bubbles*, M. Ackermann et al., ApJ, Volume 793, Issue 1, 2014, Page 64.

Ingredients:

- Supermassive Black Hole
- Cluster of evolved and young stars
- A molecular dusty ring
- Ionized gas streamers
- Diffuse hot gas
- Powerful SuperNova Remnant(s)

The Fermi bubbles: artist's impression

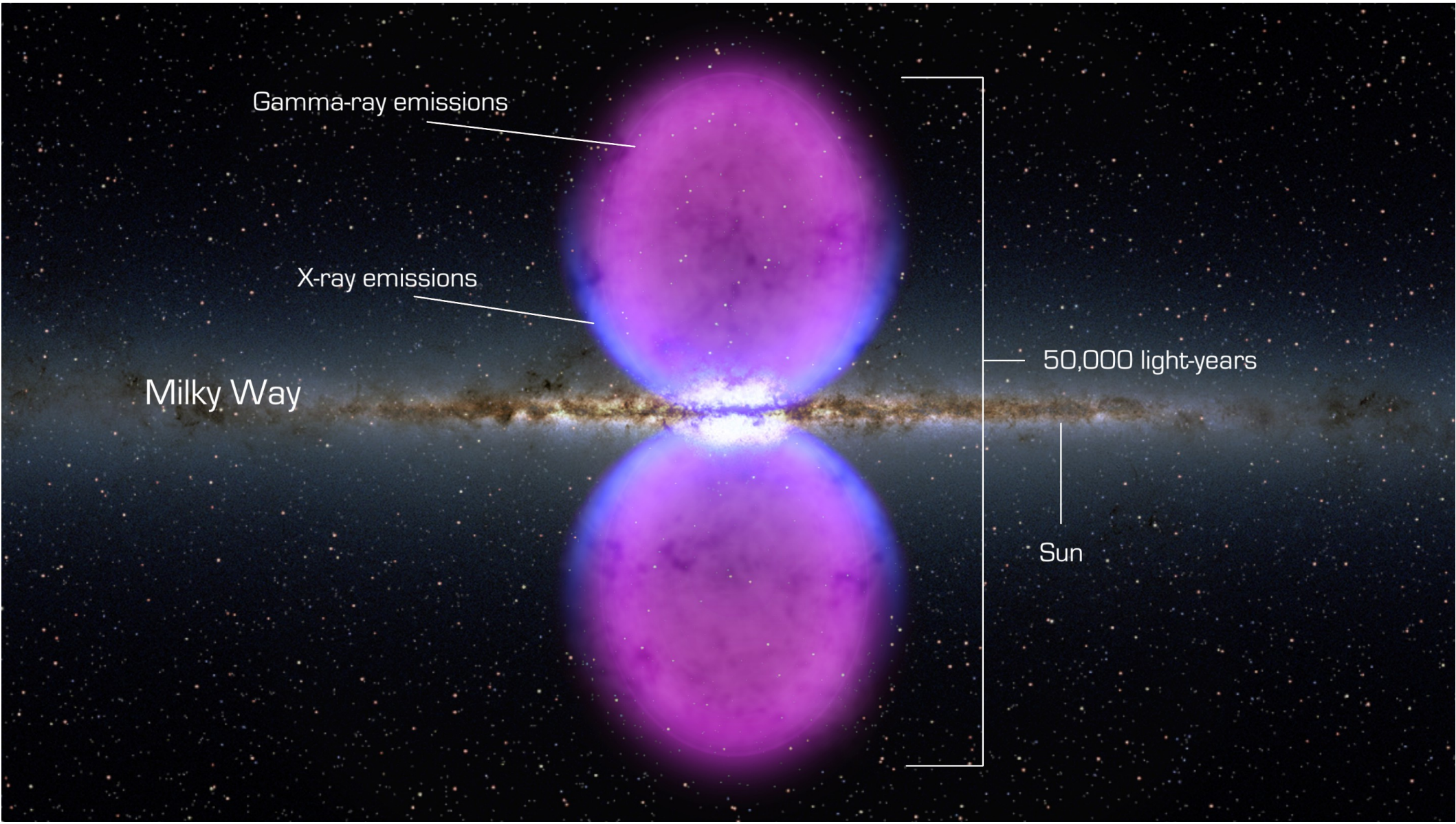

~30 mag extinction in the optical,

Much better in the NIR (JHK; e.g. 3 mag extinction in H)

The GC region: the near-mid IR view

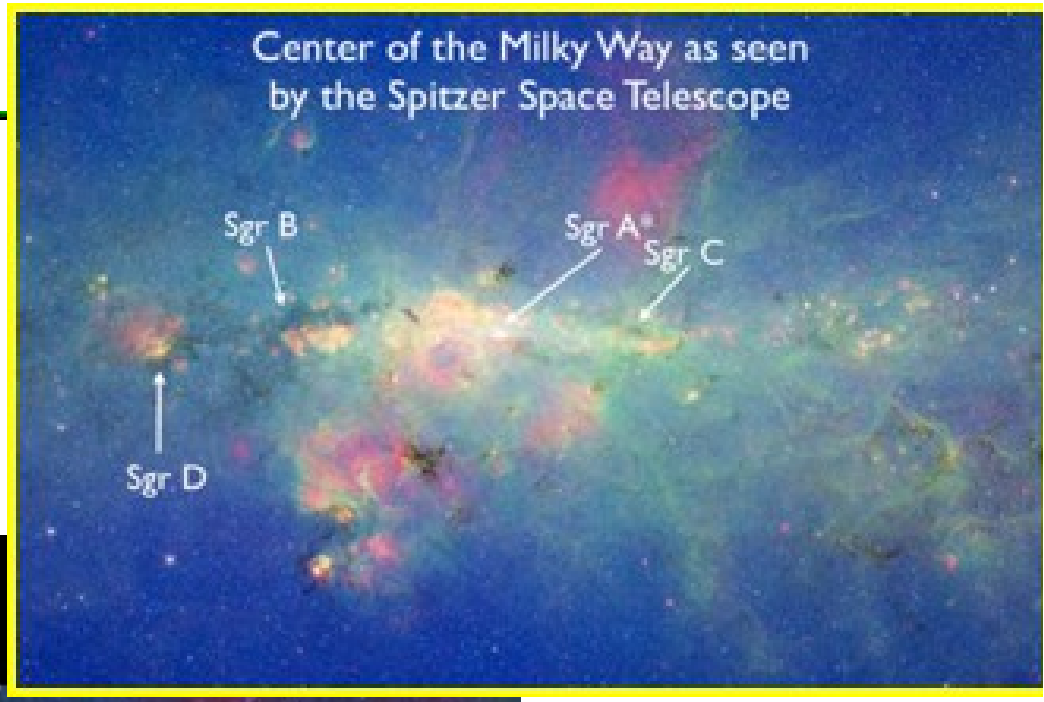

Spitzer multi λ image

The Galactic Centre: SgrA*

NASA's Nuclear Spectroscopic Telescope Array, or NuSTAR, has captured these views of the SMBH at the heart of our galaxy in the hard X-rays. The background IR image shows the location of our Milky Way's humongous BH, called Sgr A* . In the main image, the brightest white dot is the hottest material located closest to the BH, and the surrounding pinkish blob is hot gas, likely belonging to a nearby supernova remnant. The time series at right shows a flare caught by NuSTAR over two days in July. Middle panel: peak of the flare, when the black hole was consuming and heating matter up to 10^ 8 K. The main image is composed of light seen at 3 different X-ray energies. Blue: energies of 10 to 30 keV. Green: 7 to 10 keV. Red: : 3 to 7 keV. The time series shows light with energies of 3 to 30 keV. The background image of the central region of our Milky Way was taken at IR wavelengths by NASA's Spitzer Space Telescope.

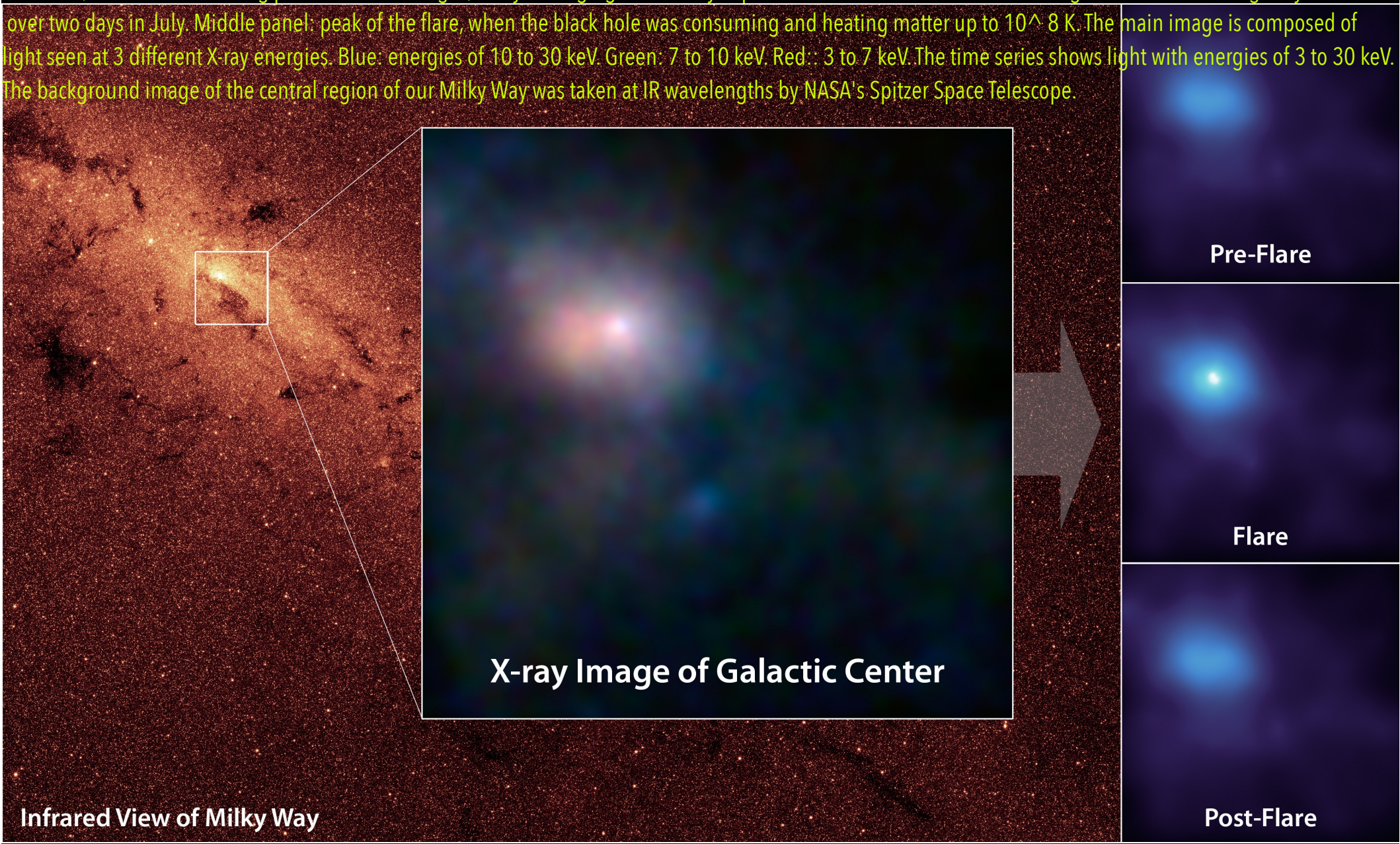

Searching for the MW "core"

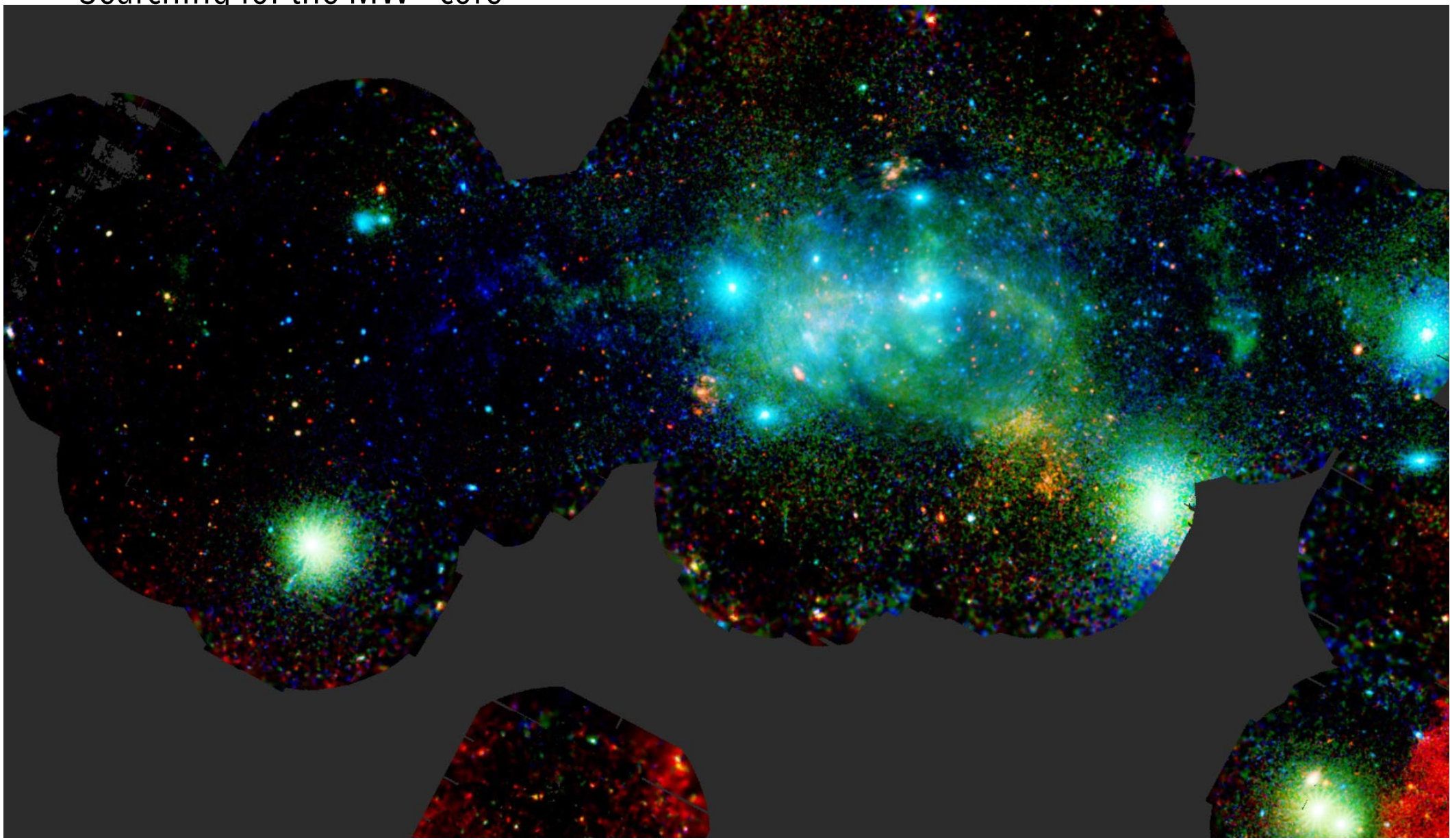

X-ray view of the central region of our Milky Way Galaxy. This image was put together in a new study by compiling all observations of this region that were performed with ESA's XMM-Newton, adding up to over one month of monitoring in total. The image combines data collected at energies from 0.5 to 2 keV (shown in red), 2 to 4.5 keV (shown in green) and 4.5 to 12 keV (shown in blue). It spans about 2.5 degrees across, equivalent to about 1,000 light-years. Image credit: ESA / XMM-Newton / G. Ponti et al. 2015

Searching for the MW "core": Chandra X – ray image (590 ks) (Muno +, 2003)

2357 point sources, 281 detected below 1.5 keV

~20 – 100 background AGNs

Muno +, 2003

TABLE 1
GALACTIC X-RAY POINT SOURCES

Object	log L_X[a] (ergs s^{-1})	Spectrum[b]	Re
MS stars[d]	25–30.3	$kT < 1$ keV plasma	
YSOs	29–31.1	$kT = 1$–10 keV plasma	
RS CVn/Algol	29–31.7	$kT = 0.1$–2 keV plasma	
WR/O stars	31–35	$kT = 0.1$–6 keV plasma	8
CVs	29.5–32.6	$kT = 1$–25 keV plasma	11,
Pulsars	29.3–39	$\Gamma = 1$–2.5 PL; $kT = 0.3$ keV BB	
NS LMXBs	31.6–38	$kT \sim 0.3$ keV BB; $\Gamma = 1$–2 PL[e]	17,
BH LMXBs	30–39	$\Gamma = 1$–2 PL[e]	
HMXBs	32.7–38	$\Gamma = 0.5$–2.5 PL	

[a] Luminosities represent ranges reported in the literature. Below $L_X \sim 10^{29}$ sources are difficult to detect, and lower bounds at this level generally represent the s limits of the respective observations.

[b] Spectra of point sources are typically described by thermal plasma (Raymond 1977; Mewe, Lemen, & van den Oord 1986), power laws (denoted by PL), or bla (denoted by BB).

[c] The references are not a complete compilation, but represent a sampling of su recent results that are amenable to comparisons with observations in the *Chandra* (0.5–10 keV).

[d] Later than type O.

[e] For the LMXBs, we include only spectral properties in quiescence ($L_X < 10^{34}$ erg

REFERENCES.—(1) Krishnamurthi et al. 2001; (2) Hempelmann et al. 1995; (3) Garmire et al. 2000; (4) Preibisch & Zinnecker 2002; (5) Kohno, Koyama, & Hamaguchi 2002; (6) Singh, Drake, & White 1996; (7) Dempsey et al. 1993; (8) Yusef-Zadeh et al. 2002; (9) Portegies-Zwart, Pooley, & Lewin 2002; (10) Pollock 1987; (11) Verbunt et al. 1997; (12) Mukai 2000; (13) Mauche & Mukai 2002; (14) Szkody et al. 2002; (15) Becker & Aschenbach 2002; (16) Possenti et al. 2002; (17) Asai et al. 1998; (18) Rutledge et al. 2001; (19) Wijnands et al. 2002; (20) Campana et al. 2002b; (21) Kong et al. 2002b; (22) Campana et al. 2001; (23) Campana et al. 2002a.

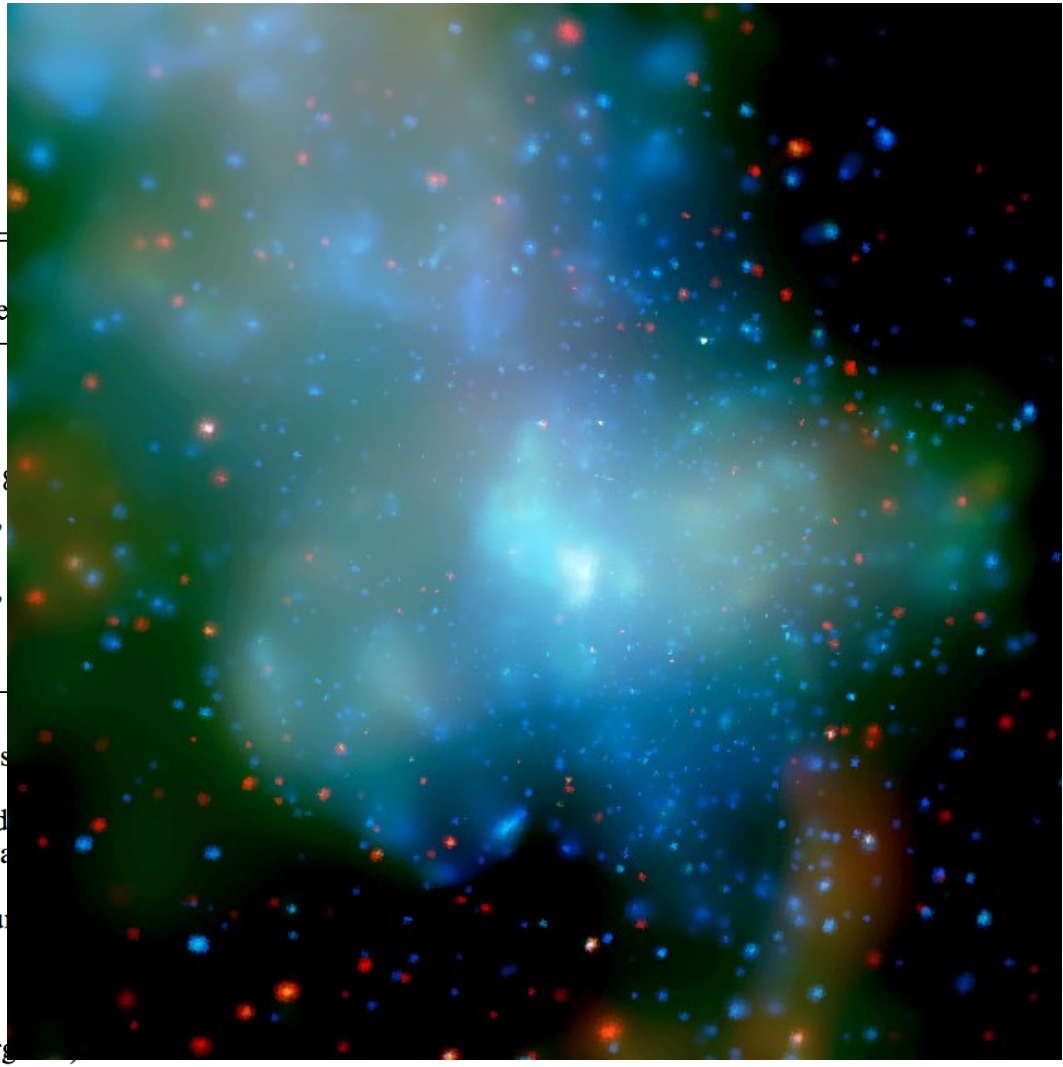

(Muno +, 2003)

Found a total of 2357 X-ray point sources.
1792 are detected in the full band,
281 in the soft band (124 in soft band only)
1832 in the hard band (441 in the hard band only).
Only 19 sources detected in all of the soft, hard, and full bands.

Such hard spectra have been seen only from magnetically accreting white dwarfs (polars and intermediate polars), wind-accreting neutron stars (pulsars)
⇒ large numbers of these systems in our field.

Absorption column toward the GC is very high (6×10^{22} cm $^{-2}$ of H)

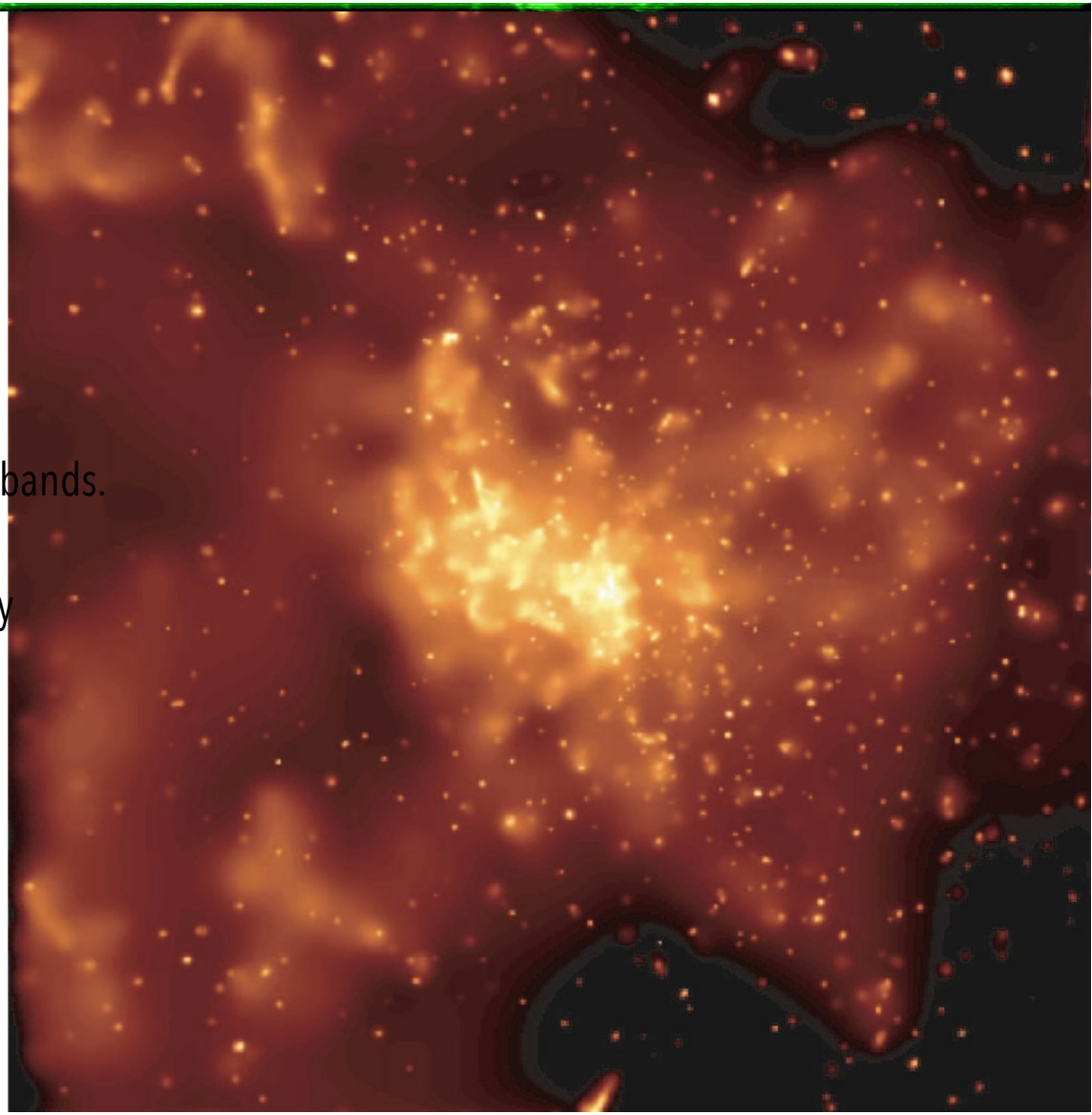

Full-band CHANDRA image of the inner 8'5 x 8'5 around Sgr A*. Image adaptively smoothed to allow point sources & diffuse emission to be easily distinguished. Logarithmic color scale is logarithmic and has been stretched to highlight the point sources.

Very few sources at the Galactic Center can be detected below 1.5 keV.

Radio emission is OK

Various components:

Sgr E: several compact HII regions (Listz, 1992)

Sgr D: HII region + SNR

Sgr C: several HII regions + non-thermal filaments (Listz & Spiker 1995)

Sgr B: (see next slide)

Sgr A :

No HI emission within 4 pc

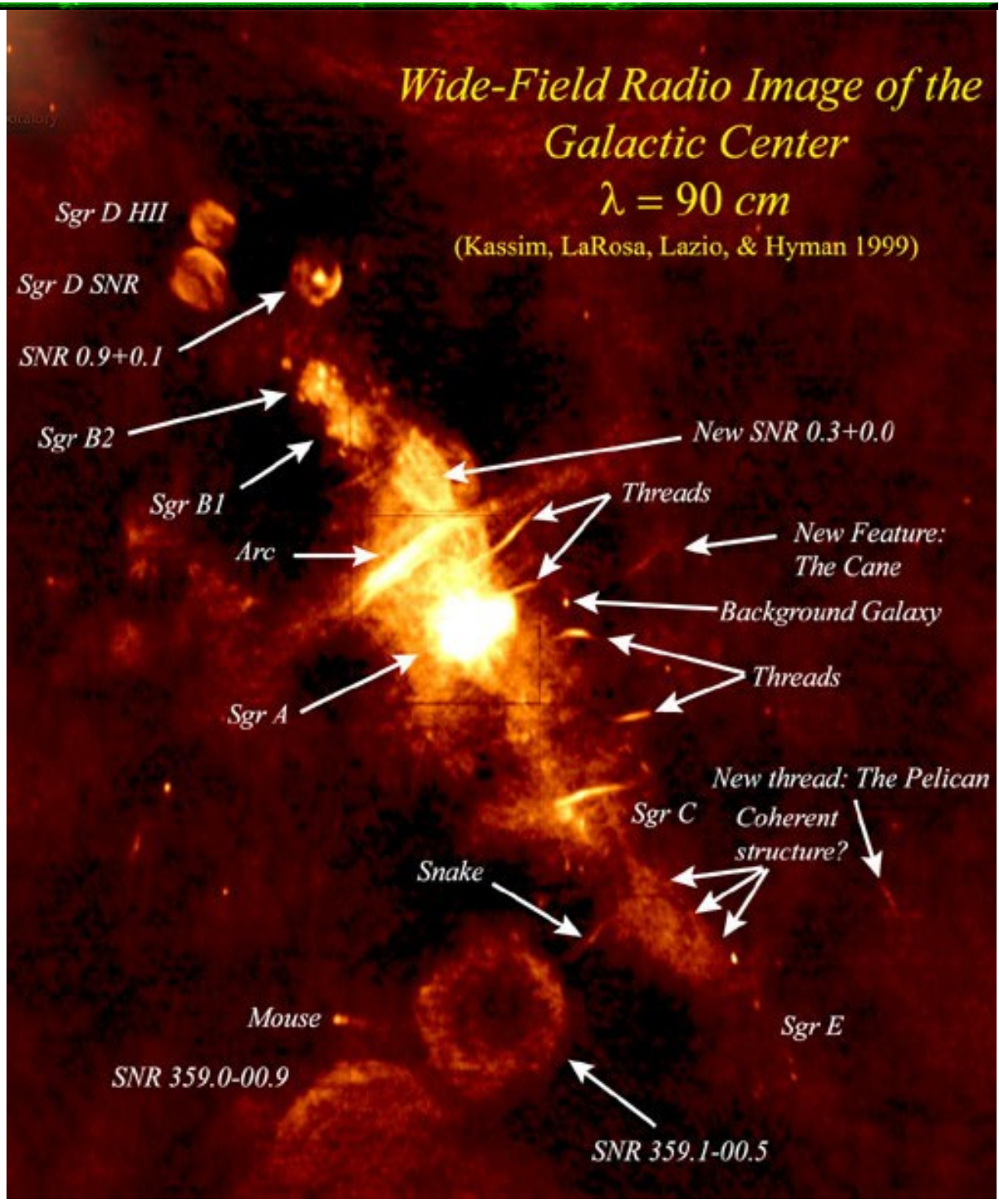

SgrB2 is a GMC @ ~ 120 pc from SgrA*, ~45 pc in size, M ~3 x 10^6 $M_\odot$, n ~3 x 10^3 cm^{-3}

The GMCloud has three main cores:

- north (N),
- middle or main (M) and
- south (S).

N & M are actively star forming

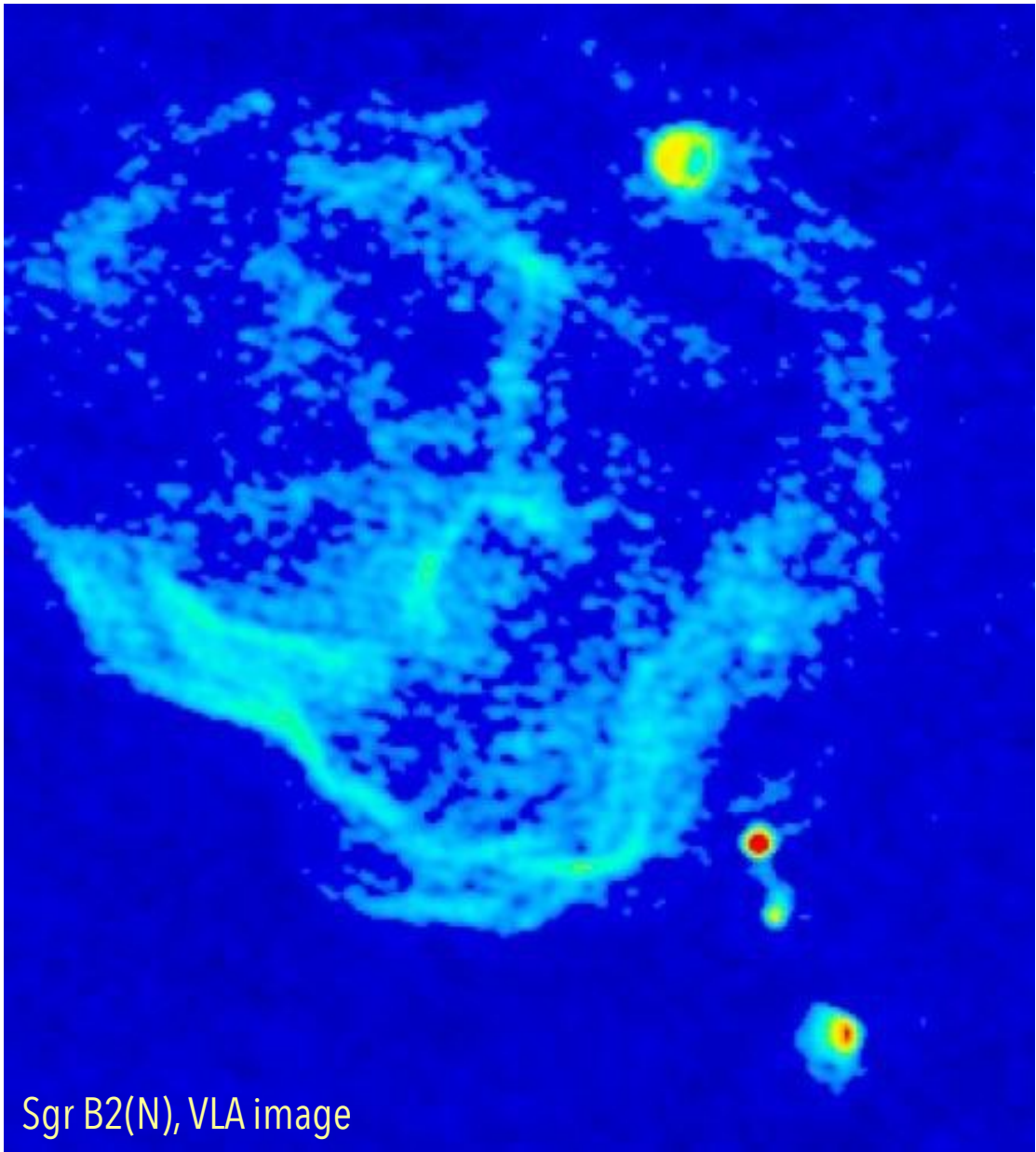

Sgr B2(N), VLA image

Radio image at $\lambda = 20$ cm

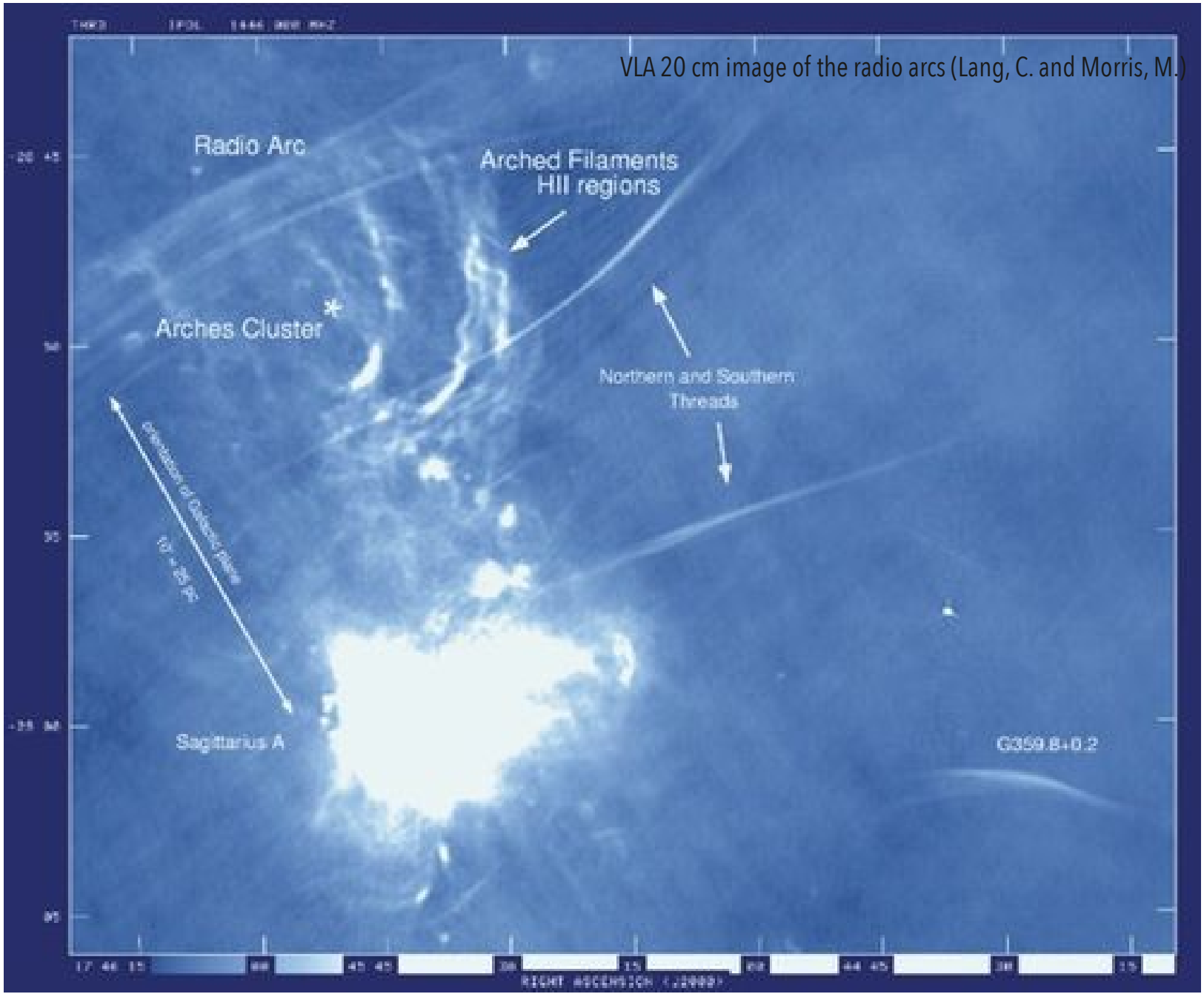

Ionizied gas and dust emission

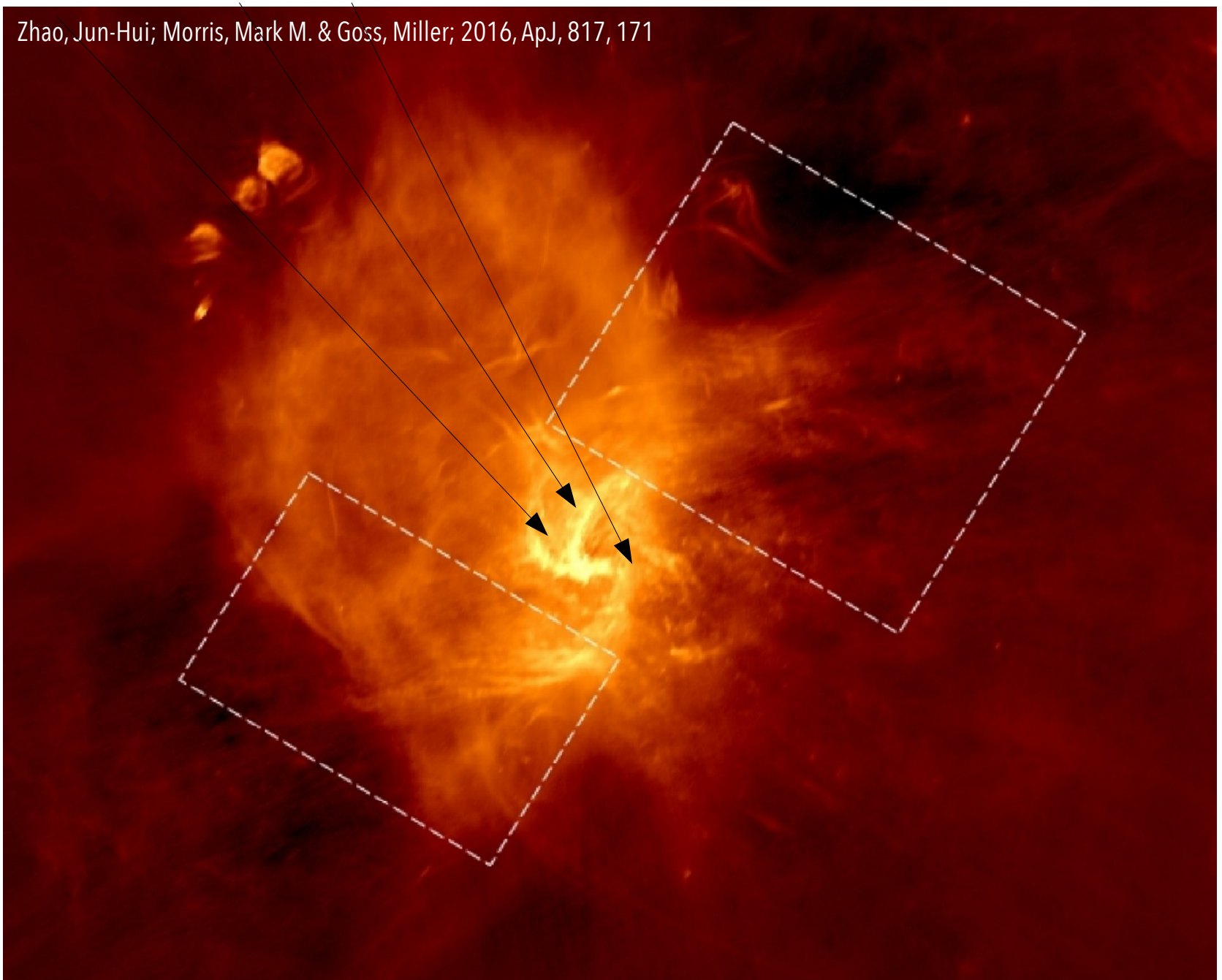

Radio emission is transparent

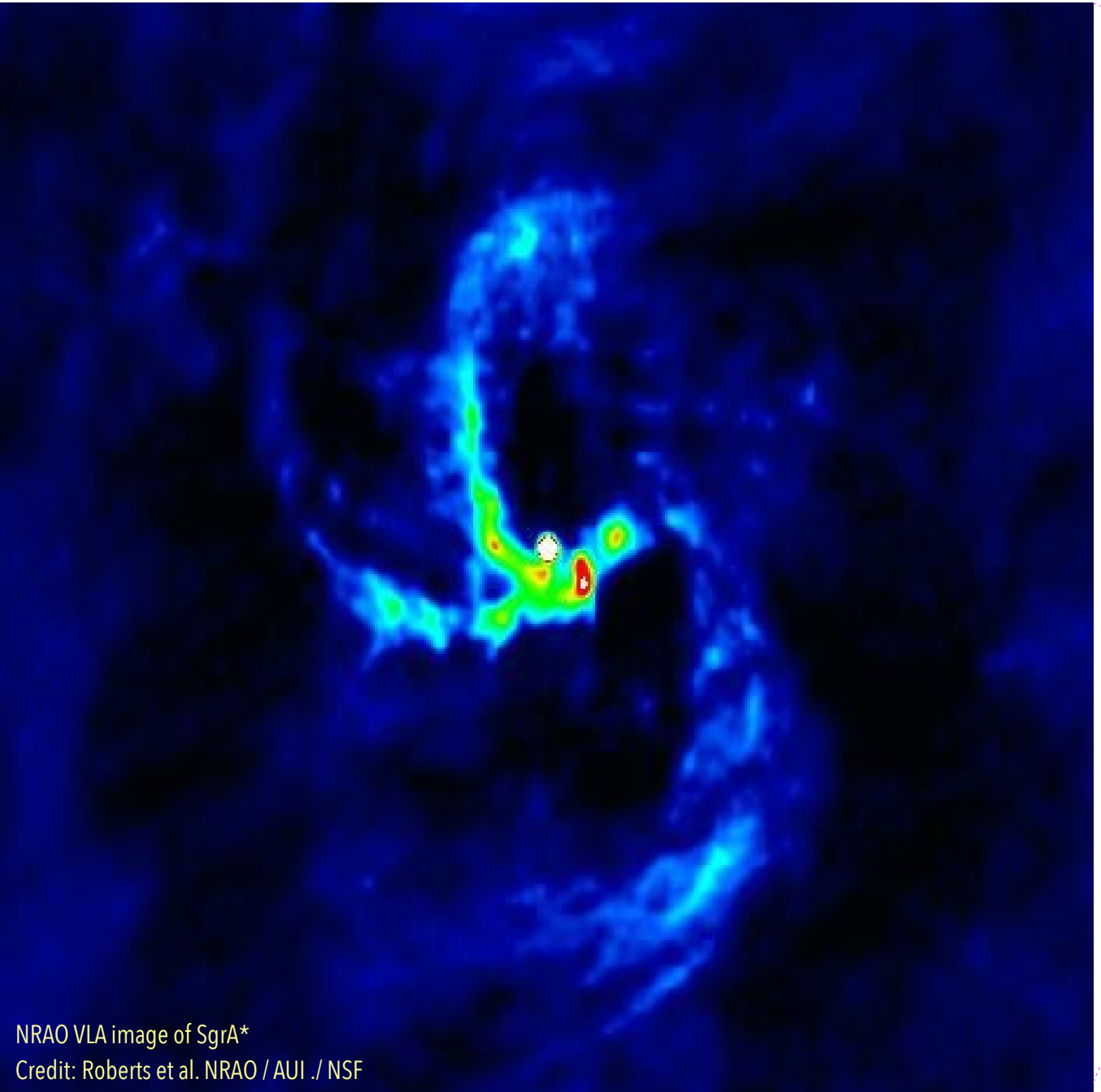

NRAO VLA image of SgrA*
Credit: Roberts et al. NRAO / AUI ./ NSF

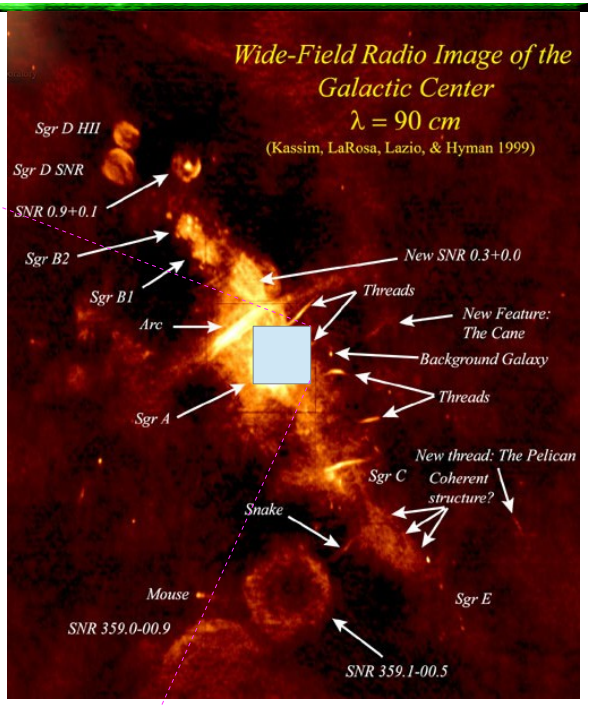

The LOS is ~ transparent to radio emission!

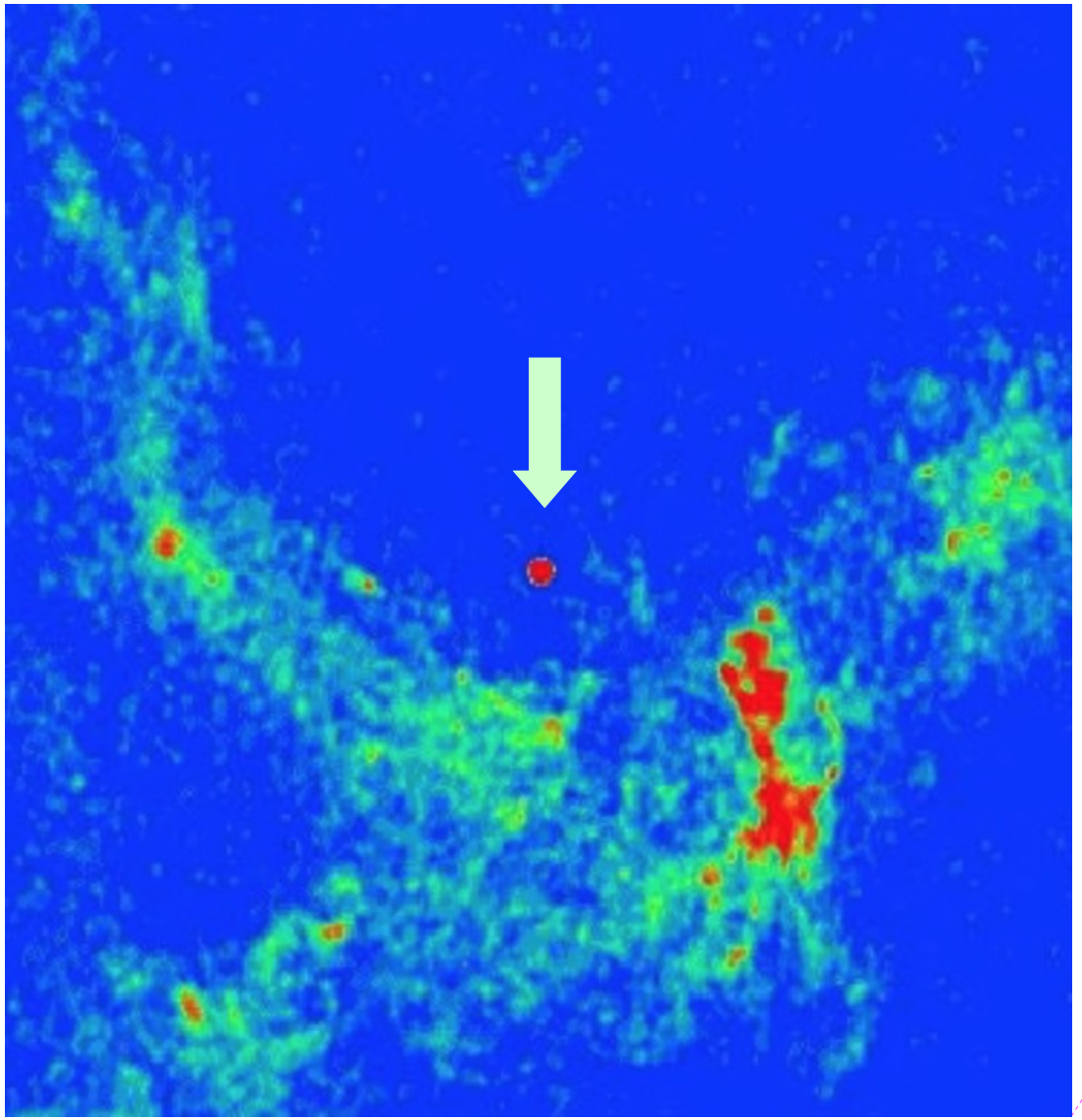

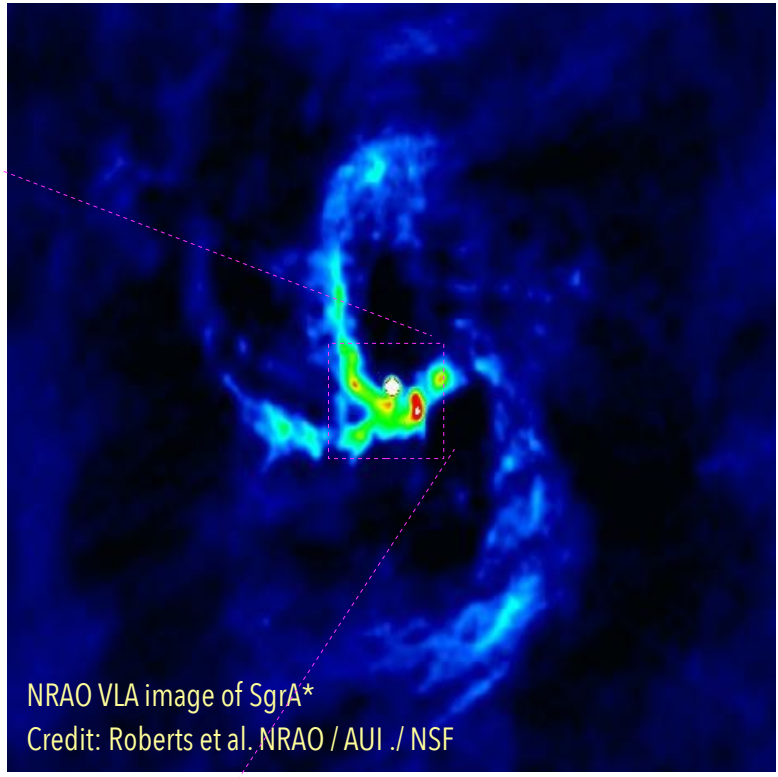

NRAO VLA image of SgrA*
Credit: Roberts et al. NRAO / AUI ./ NSF

The false-color (left) of the radio wave emission covers the inner 10″ (0.4 pc) of the Milky Way. The compact radio source Sgr A*, most likely a SMBH, is the bright red spot at the center. Diffuse green-red emission strongest to the south of Sgr A* is from ionized gas likley spiraling inwards.

Baganoff 2003 :

Overlay between X-rays & Radio emission

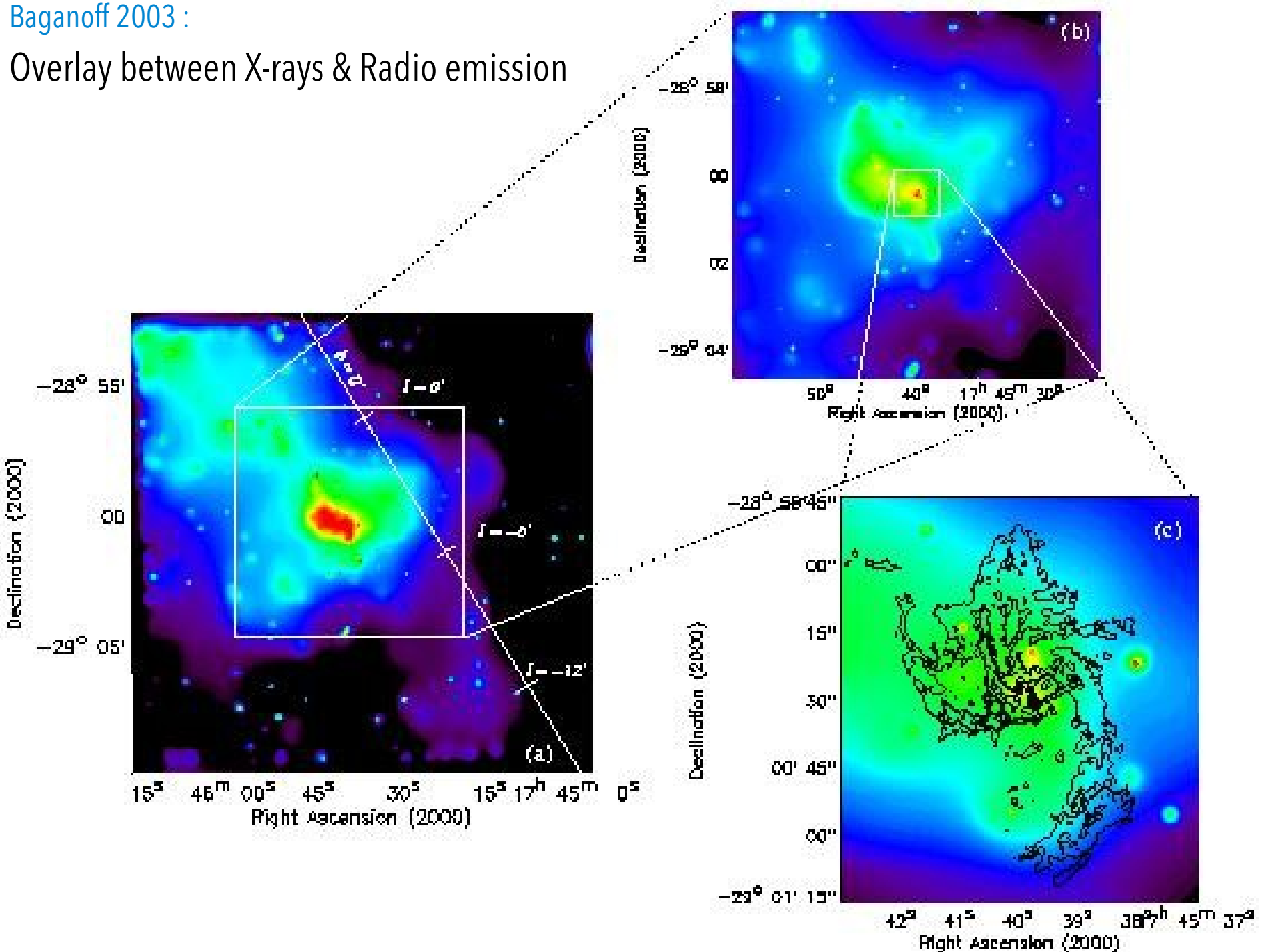

Cool (molecular) gas in the proximity of SgrA* (green/blue).

Also hot (ionized) plasma is present (red)!

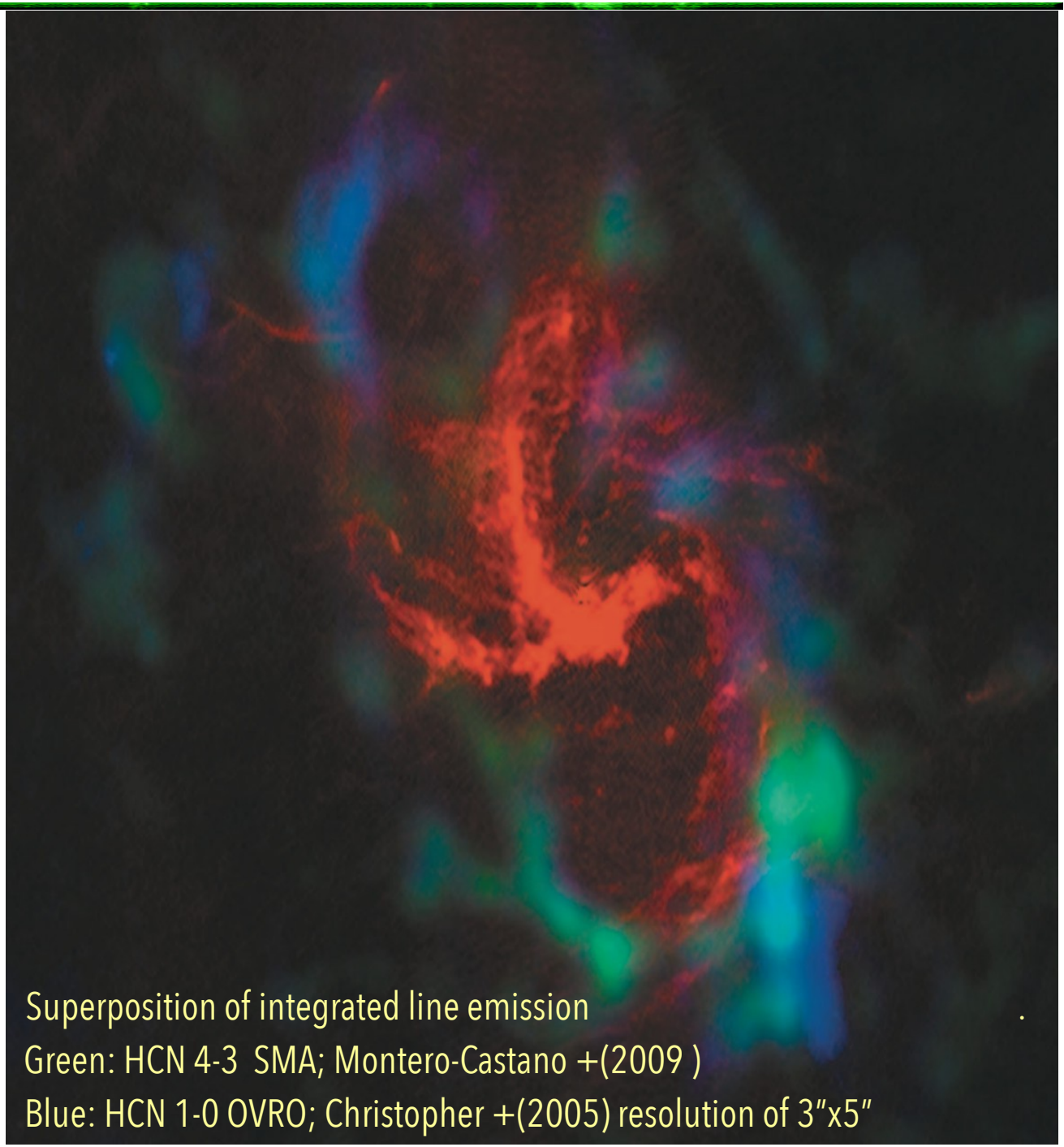

Superposition of integrated line emission
Green: HCN 4-3 SMA; Montero-Castano +(2009)
Blue: HCN 1-0 OVRO; Christopher +(2005) resolution of 3″x5″
Red: radio continuum, e.g. Yusef-Zadeh+ (2010) resolution 1″

Typical paradigm in spiral galaxies:

- In the bulge, HIM is the dominant part of the ISM
- Often, HI images of spirals show little/no WNM in the inner kpc
- Star formation in spirals occur in spiral arms where the CNM (dust & molecular gas) is dense and cold enough to start the gravitational collapse.
- Stellar byproducts and endproducts with limited living times are typically found in SFR, i.e in spiral arms
- ..... In the center of the MW, there are signatures of substantial amount of molecular gas as well as active star formation!

Yusef-Zadeh +, 2015

"Signatures of young star formation activity within two parsecs of SgrA*"

- Detected 13 H_20 masers --> self – gravity enough to overcome tidal shear by the central SMBH
- SED modeling of 64 IR-excess sources consistent with a number (at least 19) of massive YSO candidates interior to the molecular ring. ~ 260 $M_\odot$ in these objects implying a SFR of 10^{-2} $M_\odot$ / yr (after assumption of IMF)
- Detected several Si0 maser clumps, consistent with shocked proto – stellar outflows
- Measured velocities +50 / – 40 km/s, suggesting proto – stellar driven outflows with

$$\dot{M} \approx 5 \times 10^{-5} M_{SUN}\, yr^{-1}$$

- Detected radio dark clouds, i.e. cold molecular gas reservoir to feed SF activity close to SgrA*

Yusef-Zadeh +, 2015

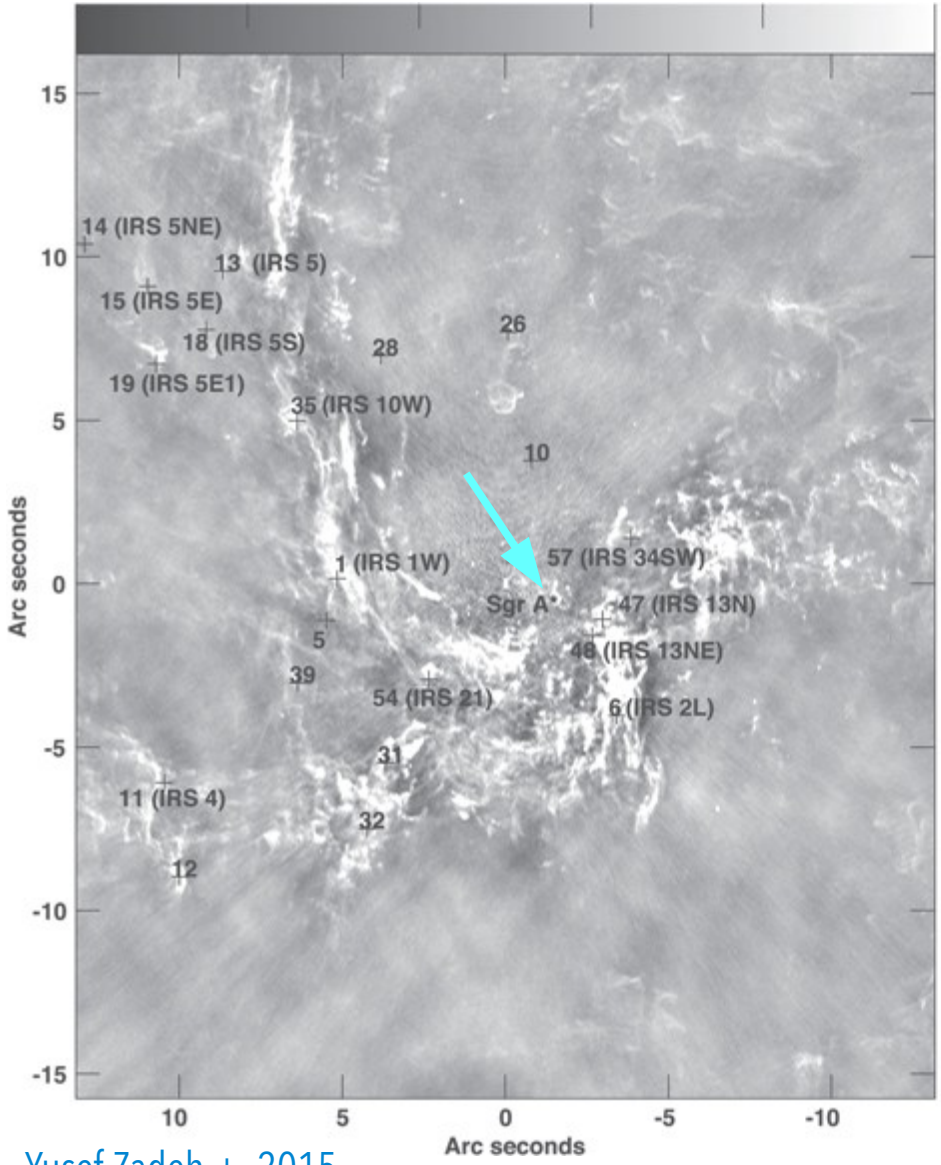

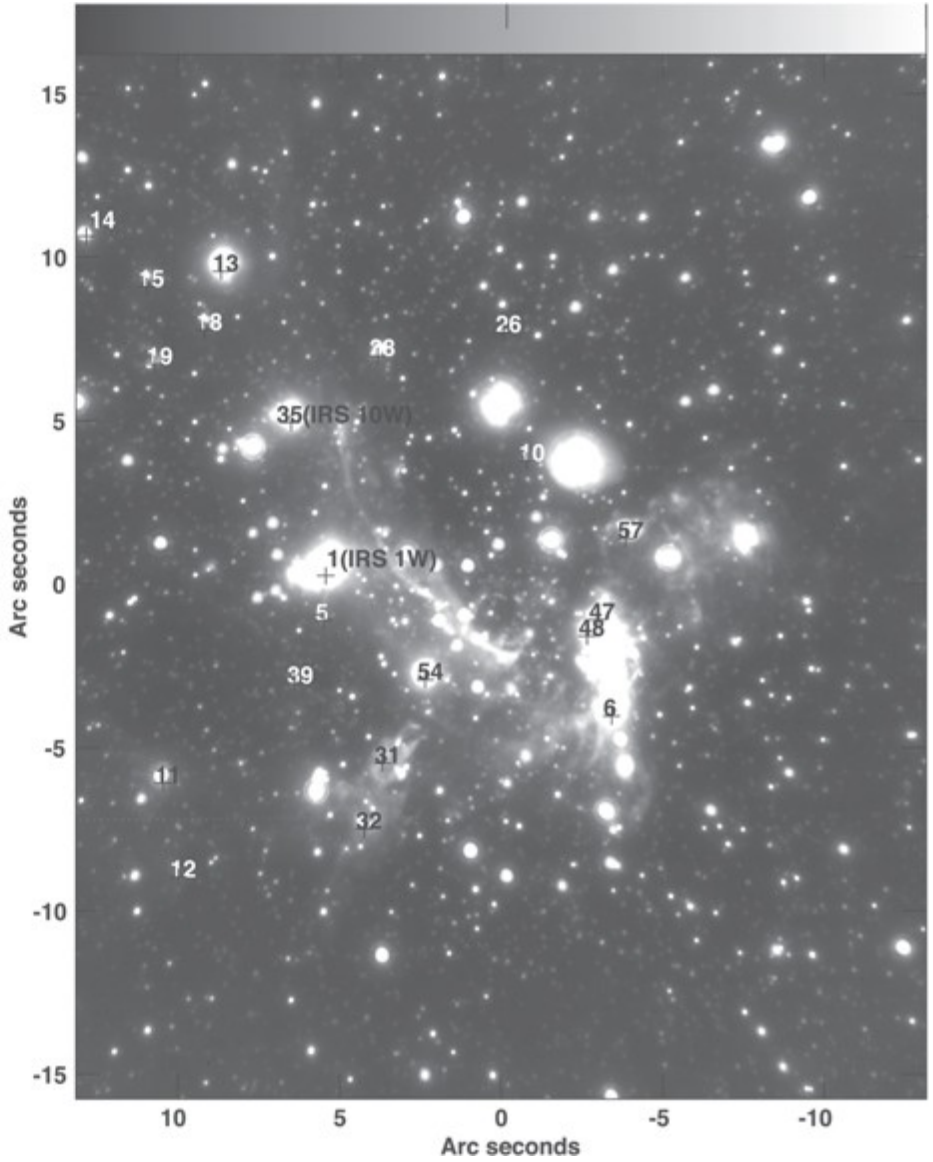

Yusef-Zadeh +, 2015

Positions of YSO candidates in a 34 GHz (left) and 3.8 μm continuum images

Radio dark clouds (Yusef-Zadeh +, 2015)

- Cold gas reservoir within 2 pc from SgrA* necessary to sustain SF activity
- There are several dark clouds consistent with cold clouds embedded in a HIM in regions where there is a deficiency of Free-Free continuum emission
- Warning: interferometric images, may suffer from "missing zero spacing flux density" introducing artificially "dark "regions around large angular scale emission.

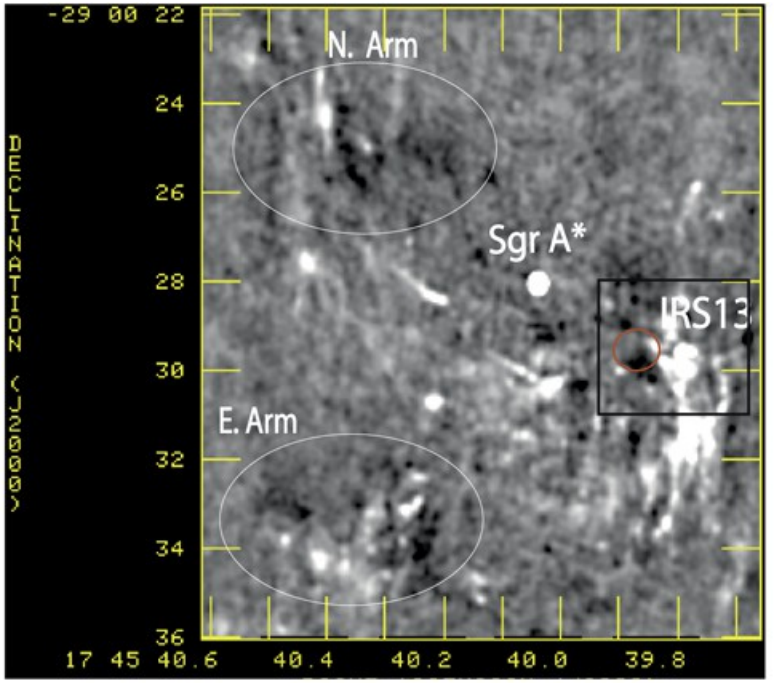

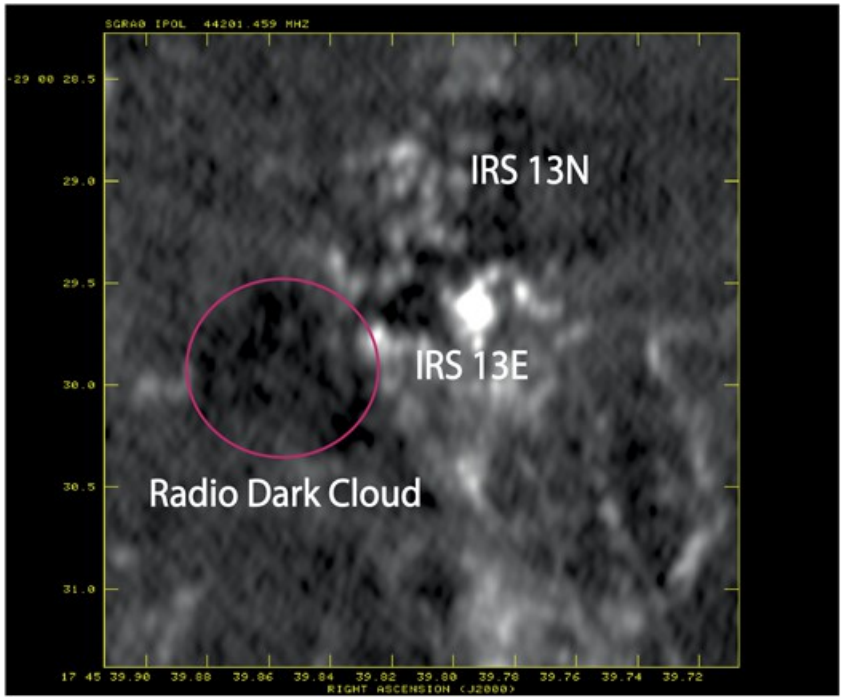

Low end SED (flux density); bars are referred to variability

Power law

Sub-mm bump (dust?)

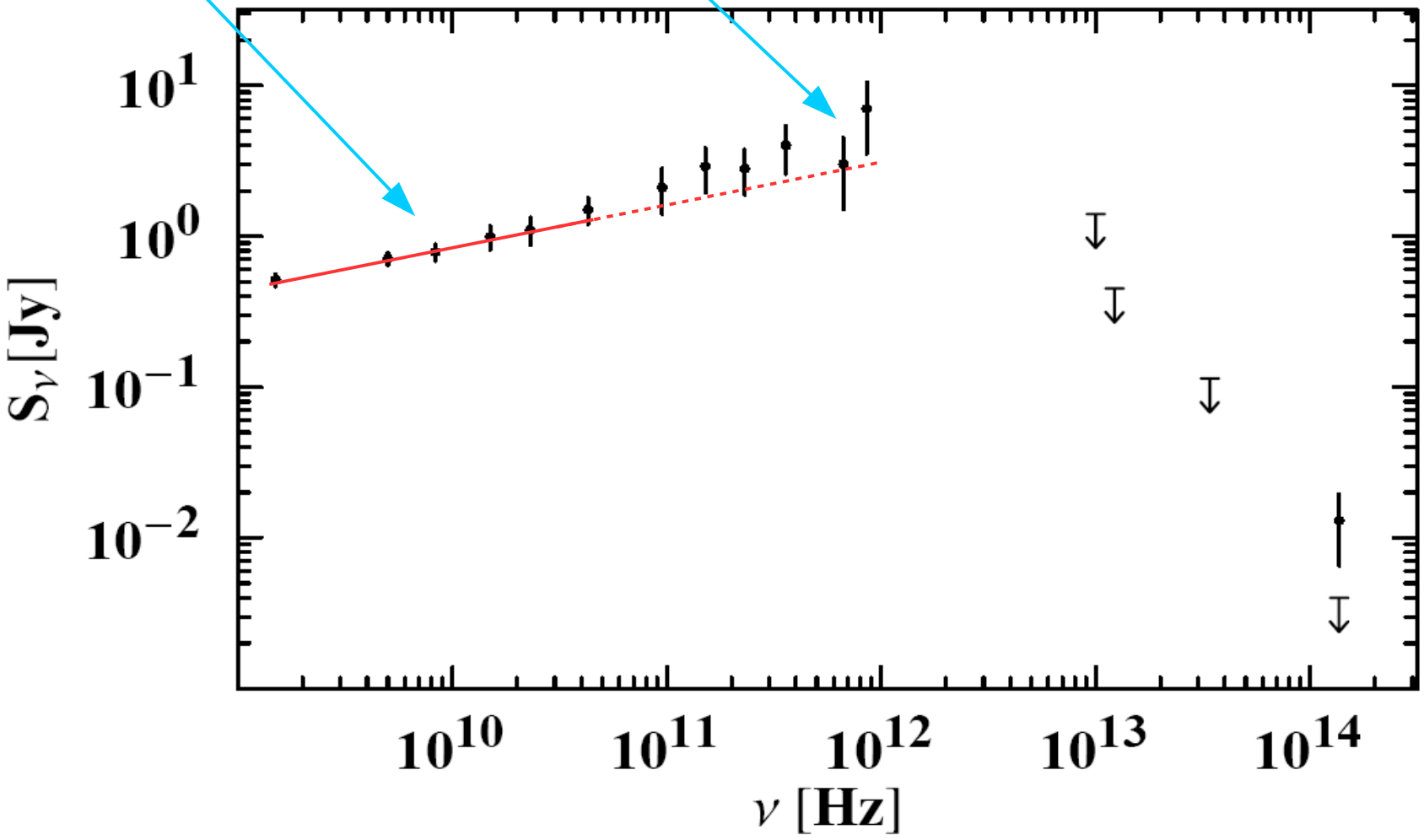

Variability.vs. frequency

Reference sources

SMA @ λ 1.3 mm observations

SgrA*

VLA @ λ1.3 & 2 cm observations

X-axis scale is "days"

Zhao et al. 2003

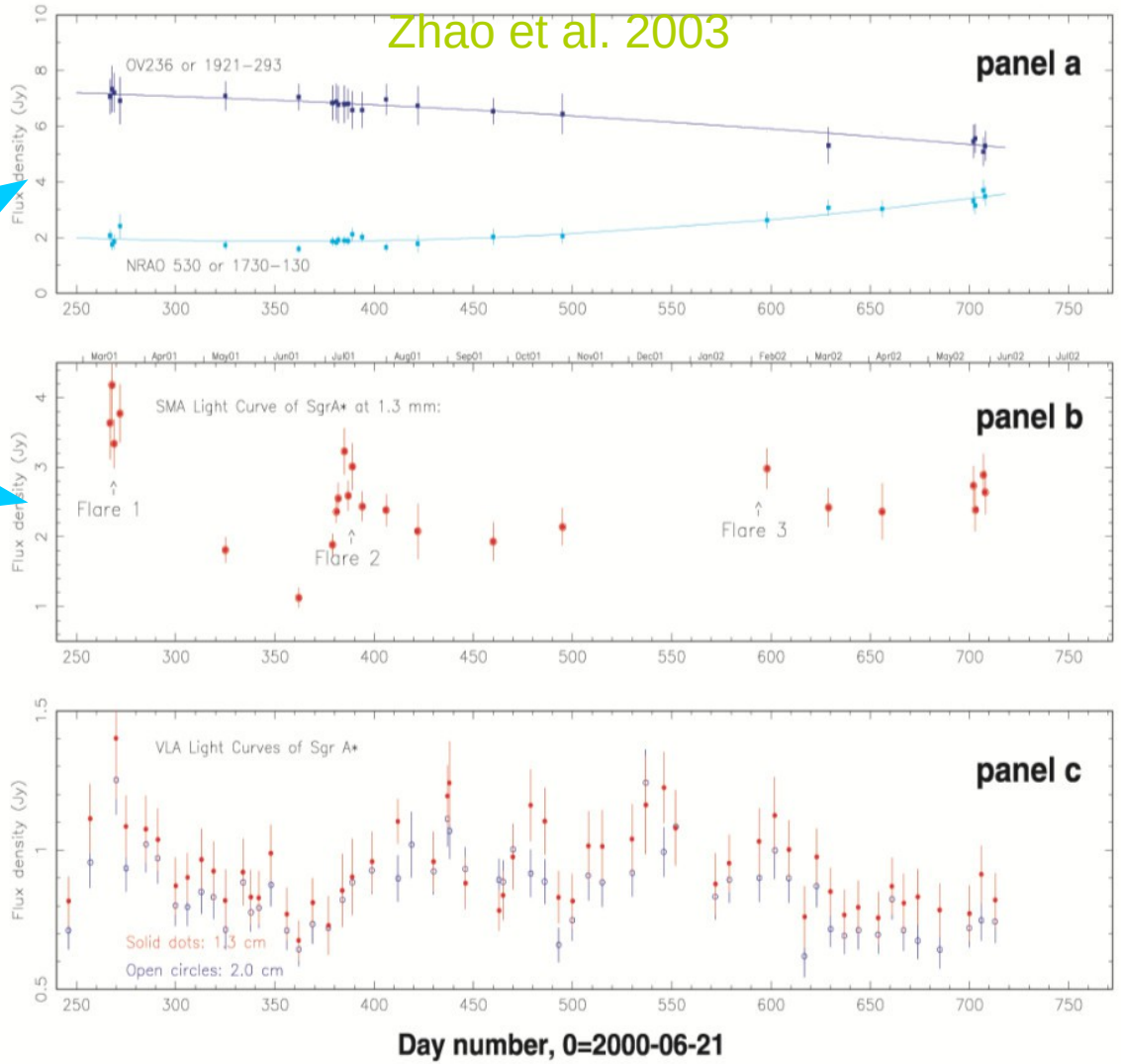

FIG. 2.—SMA light curves at 1.3 mm observed in the period between 2001 March and 2002 May for the calibrators, OV 236 and NRAO 530 (*a*) and Sgr A* (*b*). The solid curves in (*a*) are the quadratic fits to the secular variations of the flux density of OV 236 and NRAO 530. The secular trends of the flux density from NRAO 530 and OV 236 are the same as those observed at 3 mm at other observatories (e.g., M. Yun 2002, private communication). (*c*) Densely sampled radio light curves at 1.3 and 2 cm observed with the VLA (R. M. Herrnstein et al. 2003, in preparation).

Typical X – Ray variability:

The ratio between the IR-X fluxes is NOT the same, but the spectral indeces are constant ($\alpha \approx -0.6$) even if during the *bursts* (?)

Consistent with X-ray emission by *Synchrotron-Self Compton (SSC)*

Flares/bursts best seen in the X-rays, (γ-rays,) and IR.

$\Rightarrow$ a few times every day short duration

$\Rightarrow$ their nature poorly Understood

X-axis scale is "hours"

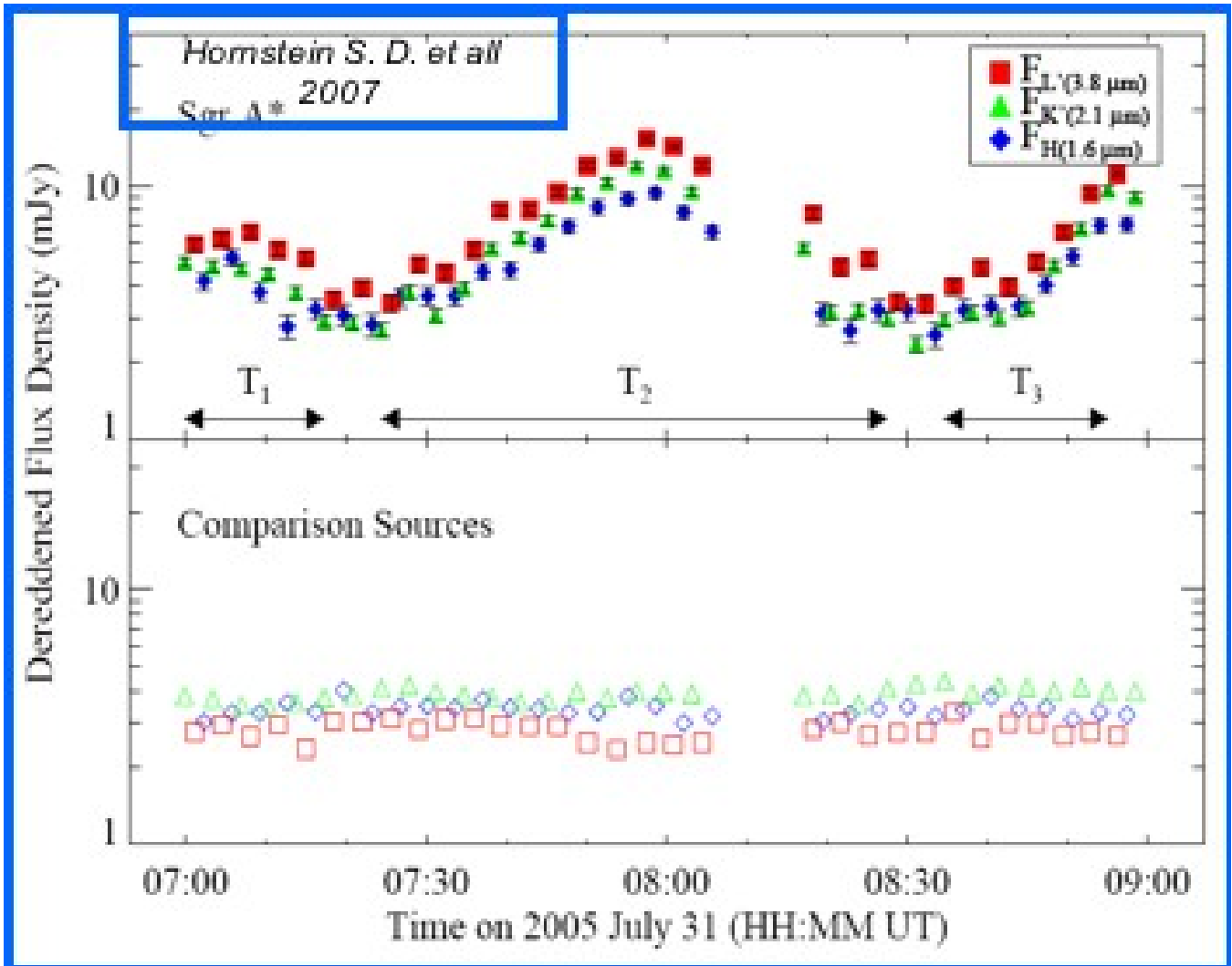

Exceptional X – Ray Variability.

Quiescent state for most of the time

Flares/bursts best seen in the X-rays, (γ-rays,) and IR.

⇒ irregular timing, short duration

⇒ their nature poorly understood (episodes of major accretion?)

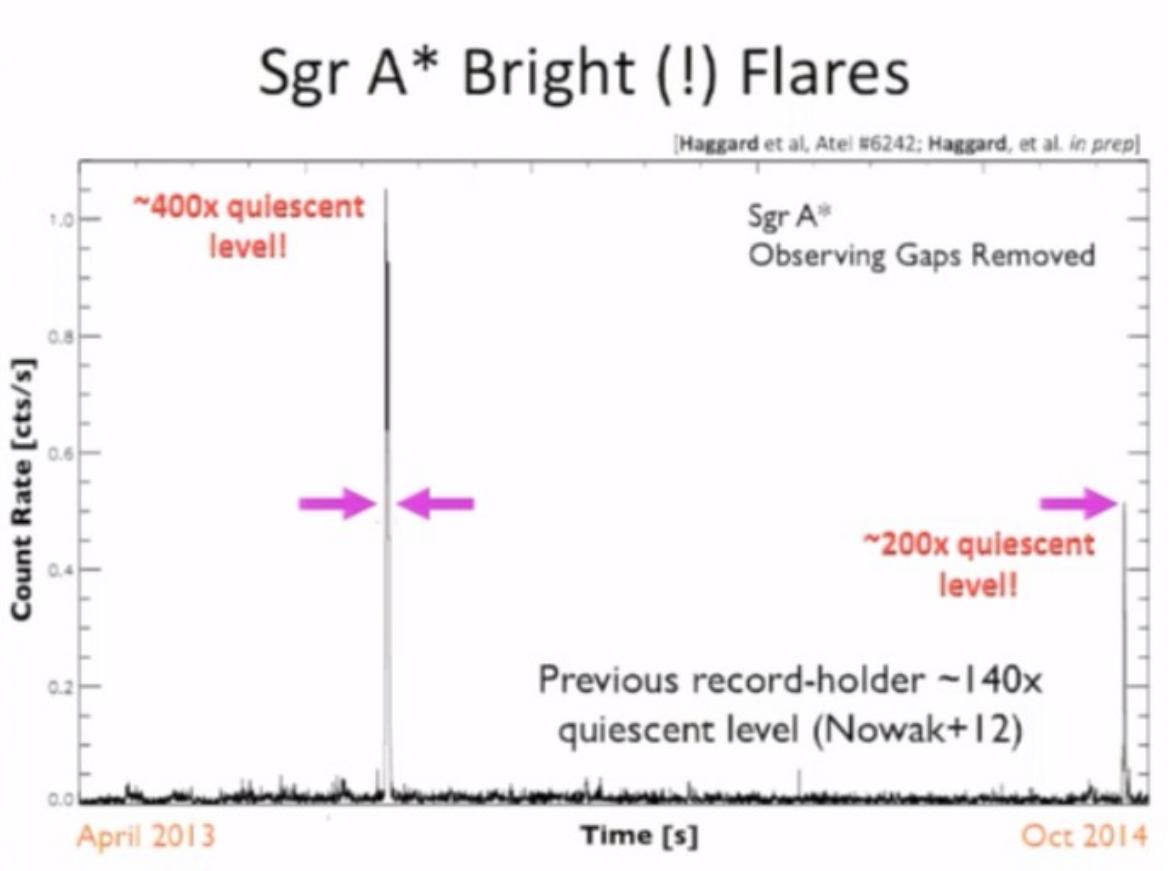

Nobukawa +, 2011

variable X – ray emission from Sgr B2

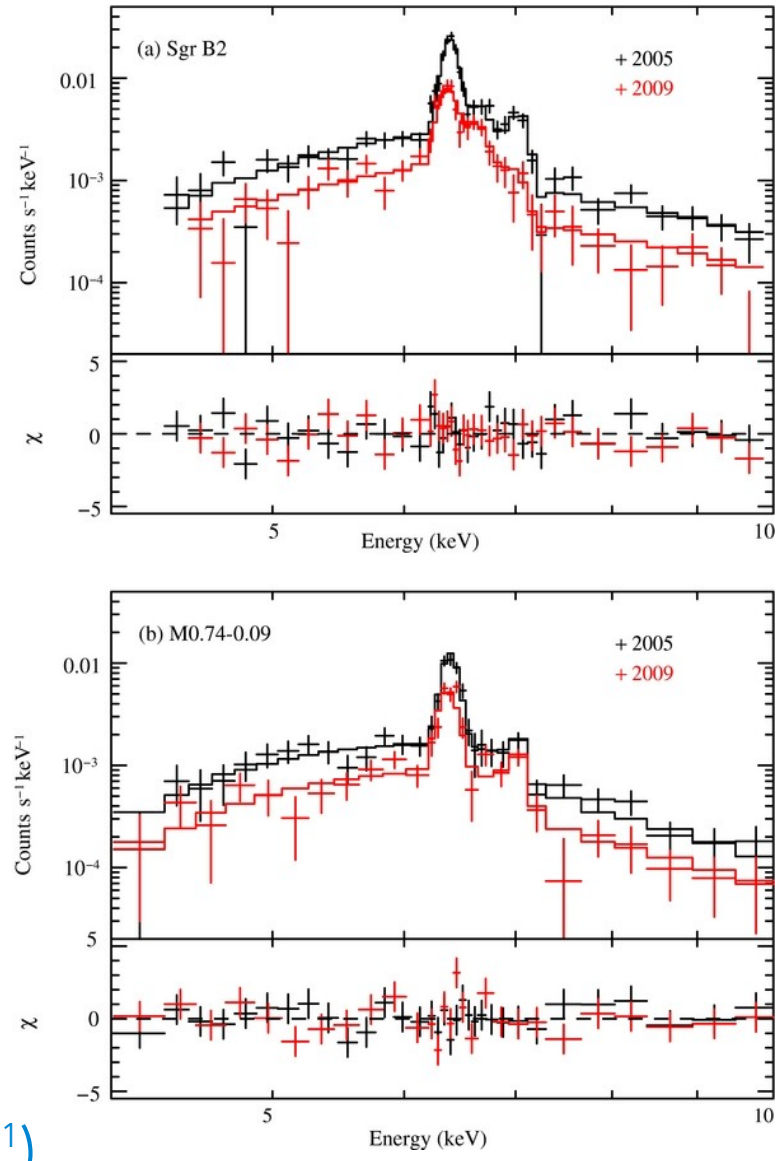

FeI Kα line emission from cold molecular gas:
the fluorescence after inner-shell ionization by

- the injection of electrons
- emission of X-rays with energies greater than 7.1 keV

- "X-ray echoes" can easily produce apparent superluminal propagation (Ponti +,2010)
- Observed X-ray luminosity of these clouds is ~10^{35} erg s^{-1}
- Illuminating object should be much brighter (>10^{39} erg s^{-1})

$\Rightarrow$ ~ 10^{6} x $L_{X\,(SgrA^*)}$ ~ 10^{33}–10^{34} erg s^{-1} (present luminosity).

Nobukawa +, 2011

variable X – ray emission from Sgr B2

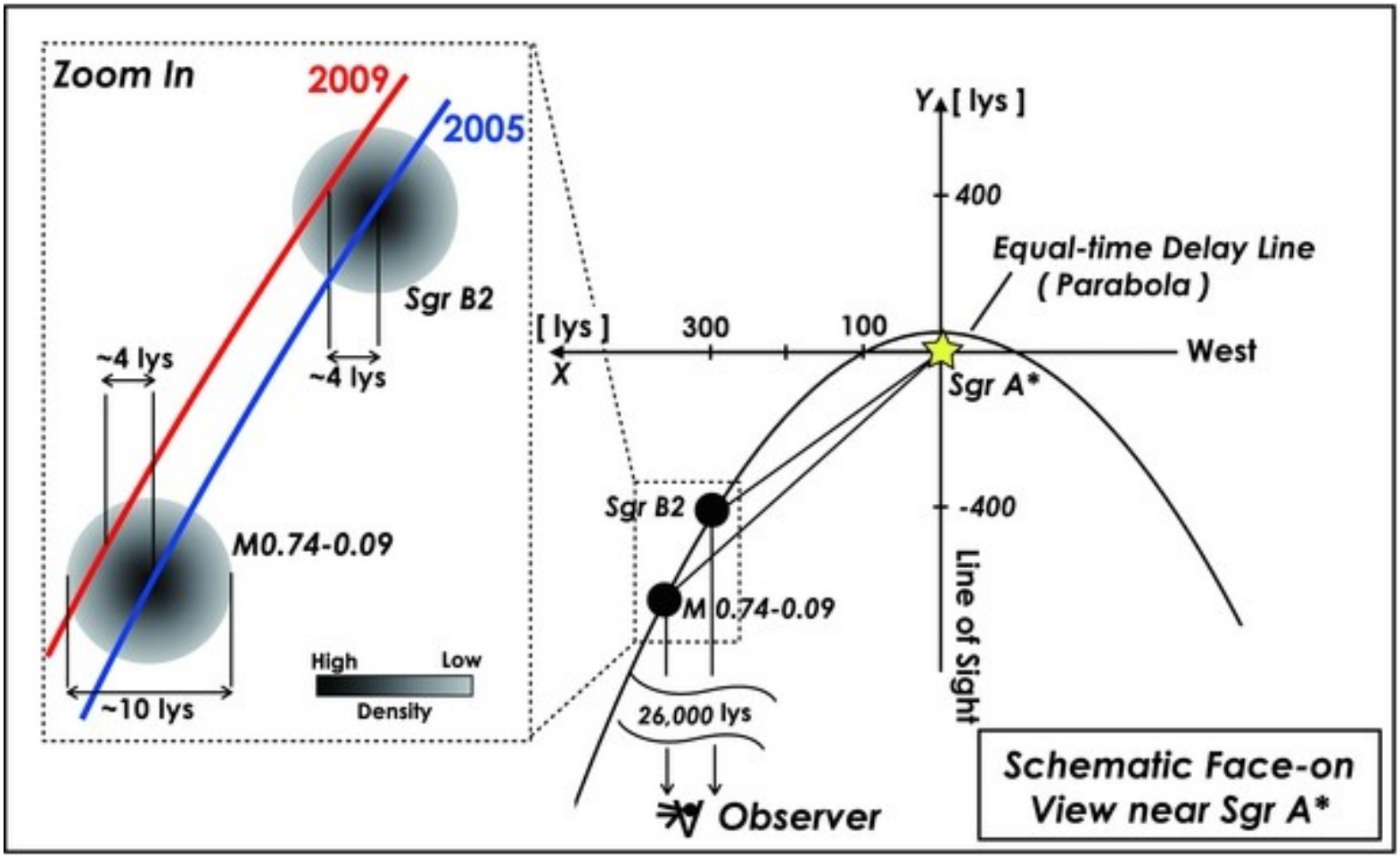

⟹ Variable X-ray activity in SgrA*, non scales much larger than present (a few 100s)

Example of typical X – ray flare: http://www.dailygalaxy.com/.a/6a00d8341bf7f753ef01b7c7a28b58970b-pi

Low end SED(energy)

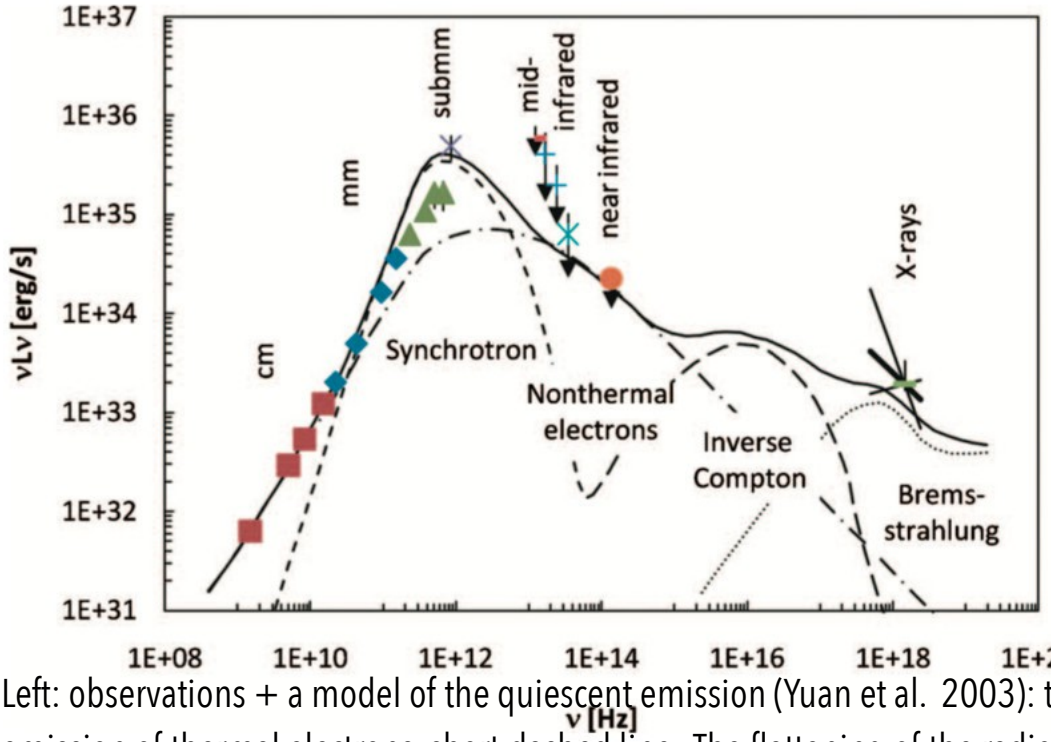

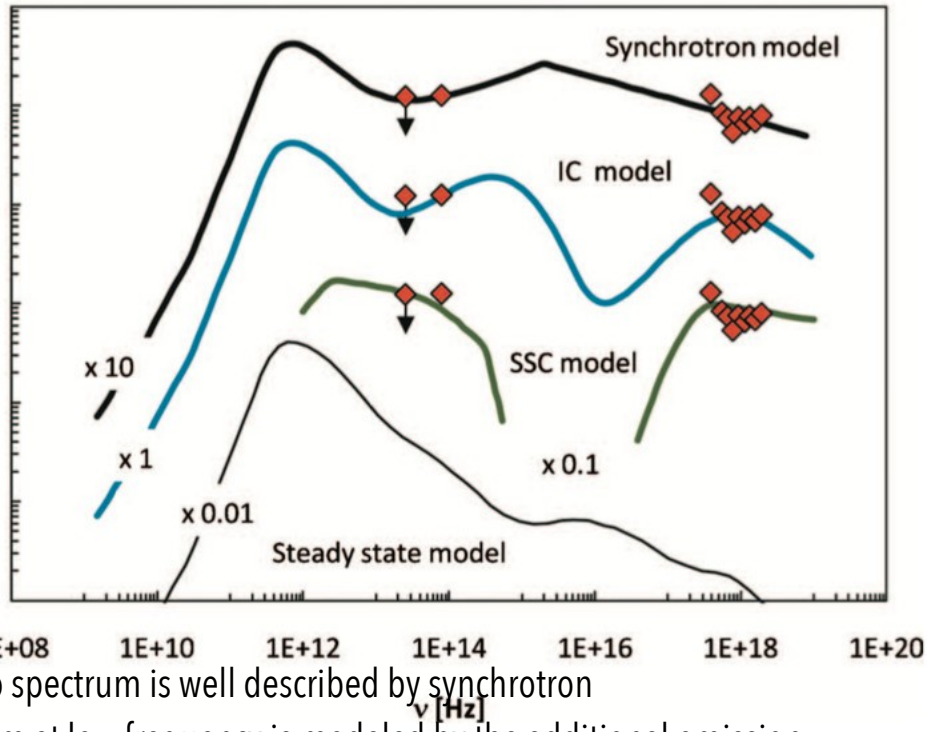

Left: observations + a model of the quiescent emission (Yuan et al. 2003): the radio spectrum is well described by synchrotron emission of thermal electrons short-dashed line . The flattening of the radio spectrum at low frequency is modeled by the additional emission from a non-thermal power-law distribution of electrons, which carry about 1.5% of the total thermal energy dash-dotted line . The quiescent X-ray emission arises from thermal bremsstrahlung from the outer parts of the accretion flow dotted line . The secondary maximum Long-dashed line at frequencies of about 1016 Hz is the result of the IC scattering of the synchrotron spectrum by the thermal electrons. Right: SED during a simultaneous x ray and IR flare: while the total energy in the radio emission is largely unaffected during a flare, the IR and x-ray fluxes increase by factors of 10 and 100, respectively from Dodds-Eden + (2009) . The near-IR emission is from synchrotron of transiently heated electrons. Several emission mechanisms can account for the x-ray flares. Top: Synchrotron model, in which both x-ray and IR emission are synchrotron radiation from a population of ultra-relativistic electrons with a power-law energy distribution. Middle: IC model, in which the near-IR emitting electrons upscatter the submm seed photons to x-ray energies (synchrotron and IC model from Dodds-Eden +, 2009) . Bottom: SSC model: near-IR emitting electrons transfer their energy to the synchrotron photons emitted from the same electron population (Sabha +, 2010).

IR Variability and stellar motions.

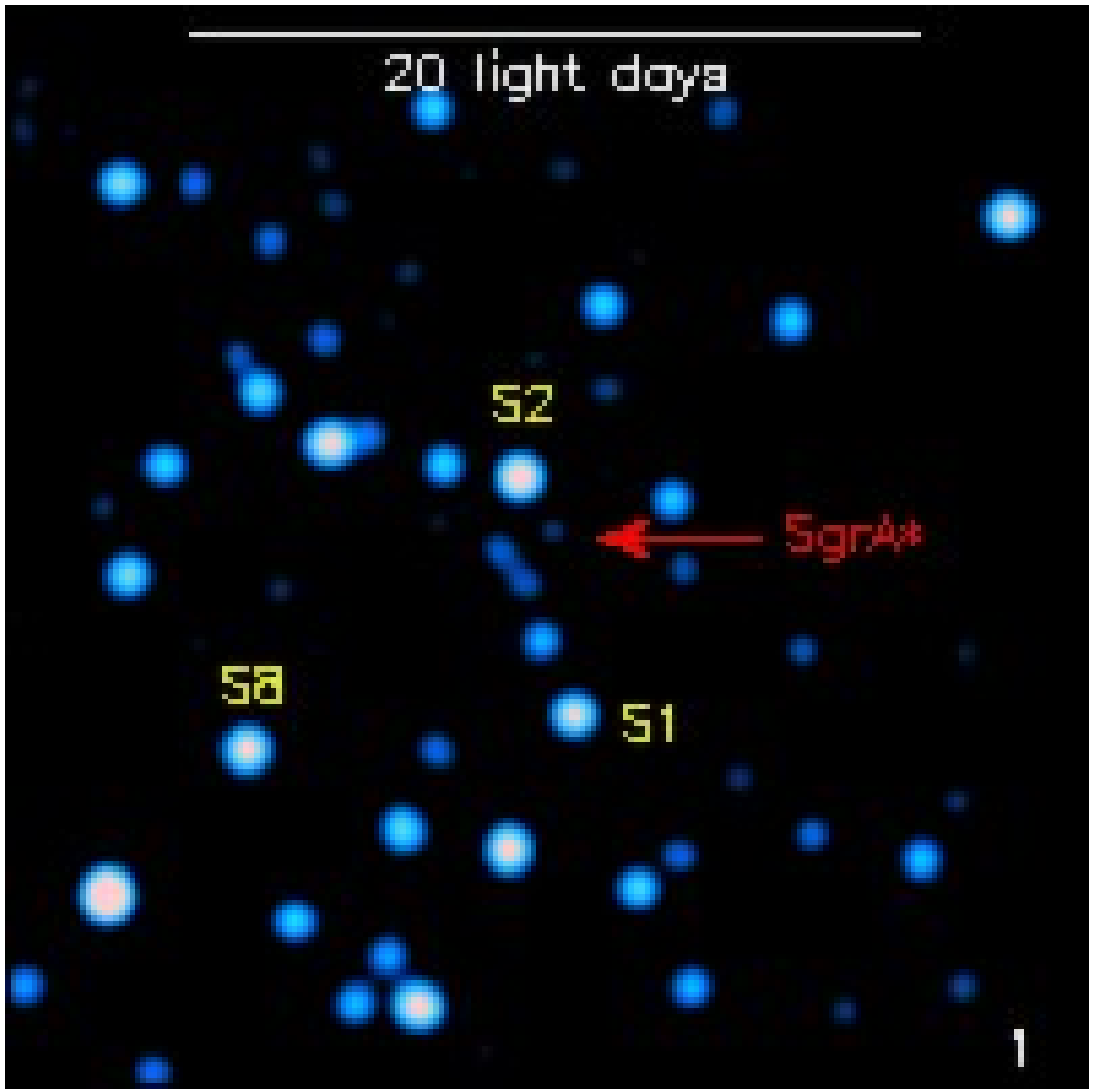

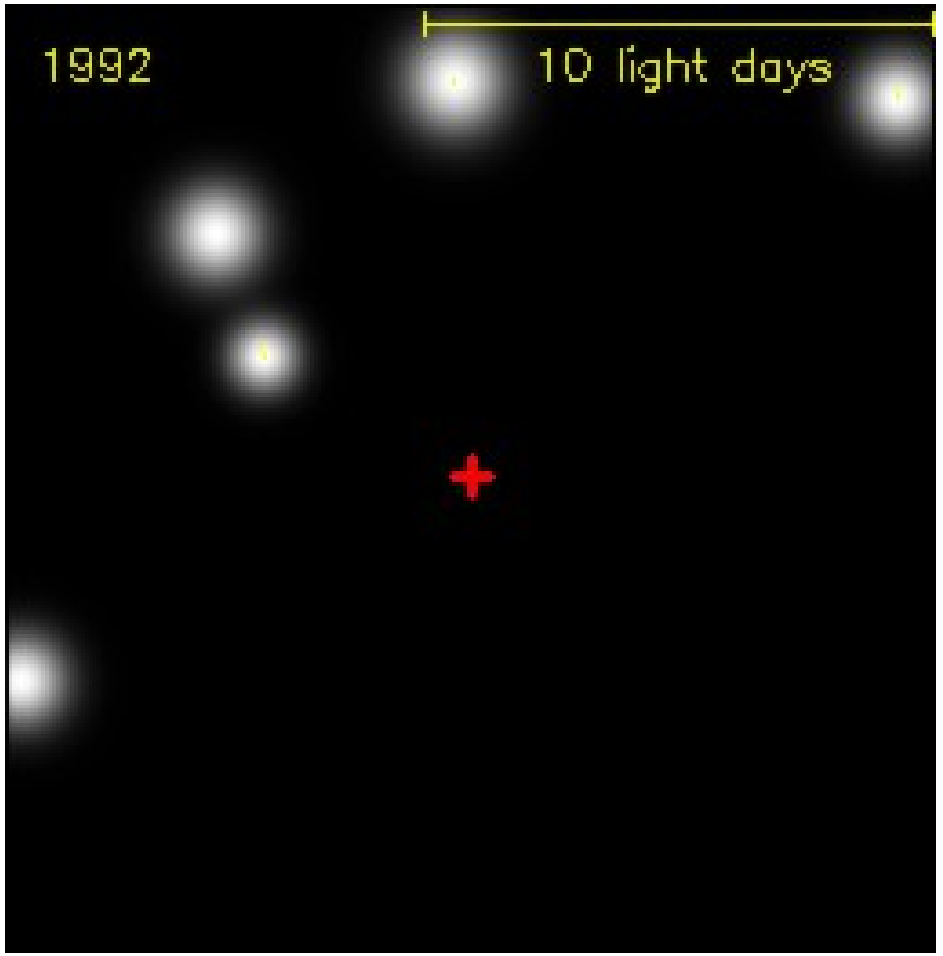

A weak "core" is often found in all (spiral galaxies

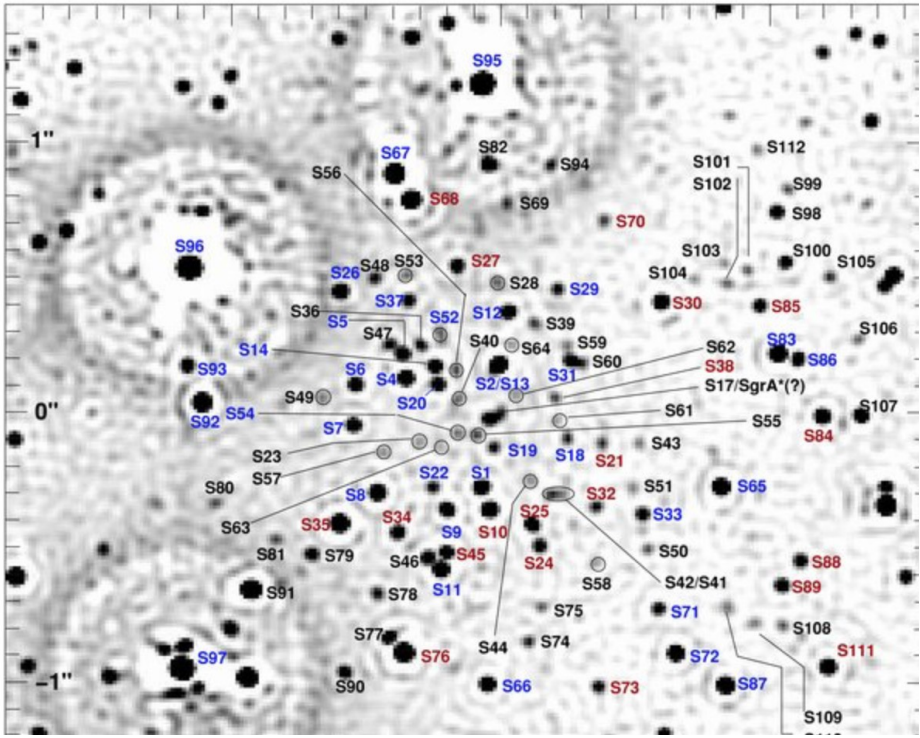

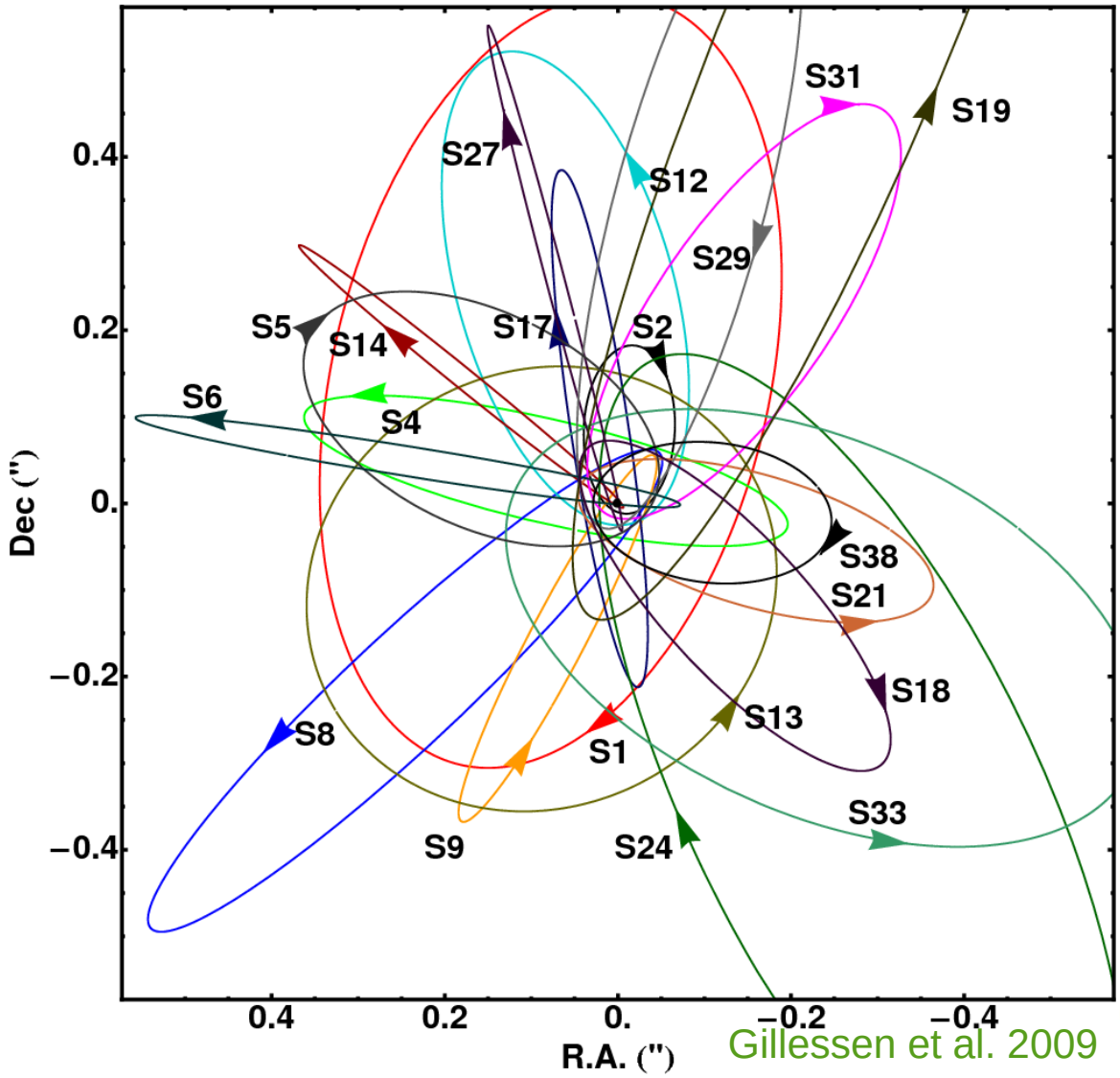

Gillessen et al. 2009

The orbit of S2 (1992-2013)

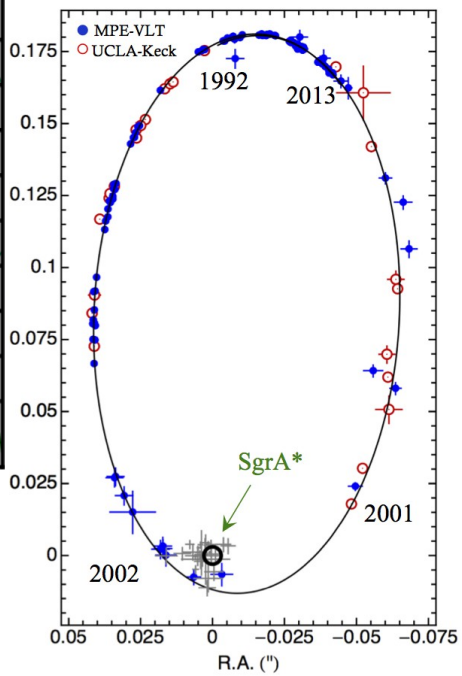

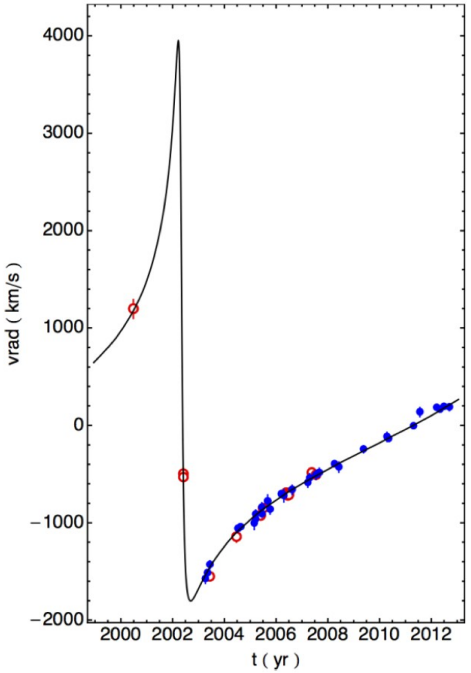

Position and apparent proper motion

Reid et al 1999:

RA(1996.25) = 17h45m40s.0409
DEC(1996.25) = – 29o00'28".118

Uncertainty 12 mas

Corrections due to solar motion, upper limit to peculiar velocity < 15 km s^{-1}

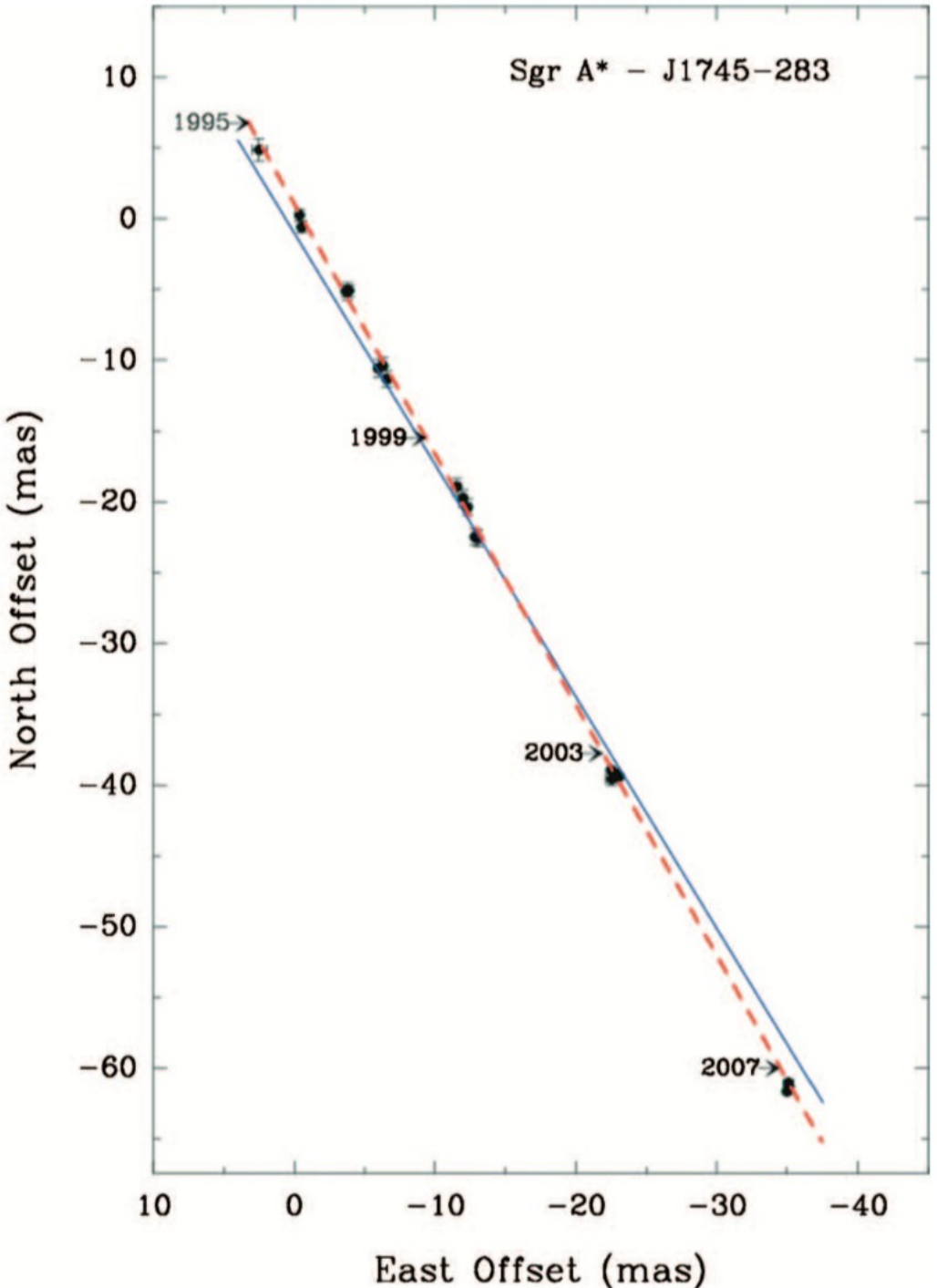

Size:

Doeleman *et al. Nature* **455**, 78-80 (2008)

Goal: resolve structures in the innermost accretion flow surrounding Sgr A*, where strong gravitational fields distort the appearance of radiation emitted near the black hole.

Earlier VLBI observations at 3.5 & 7 mm detected intrinsic structure in Sgr A*

The spatial resolution of observations at 1.3 mm is limited by interstellar scattering.

Doeleman + VLBI observations at 1.3 mm:
Size 37^{+16}_{-10} microarcseconds on the intrinsic diameter of Sgr A*.

This is smaller than the expected apparent size of the event horizon of the presumed black hole, suggesting that the bulk of Sgr A* emission may not be centred on the black hole, may arisesin the surrounding accretion flow.

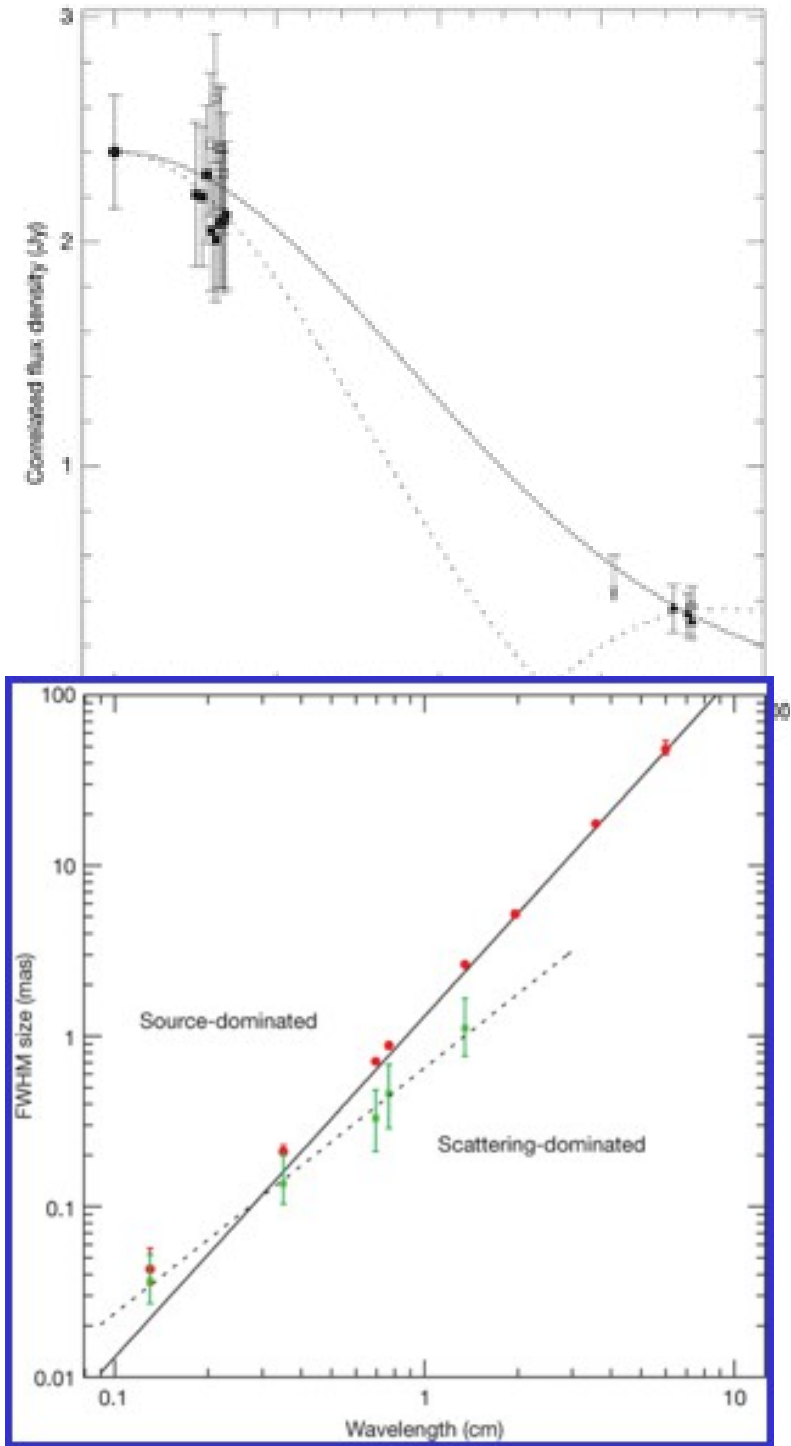

The galactic centre: SgrA*

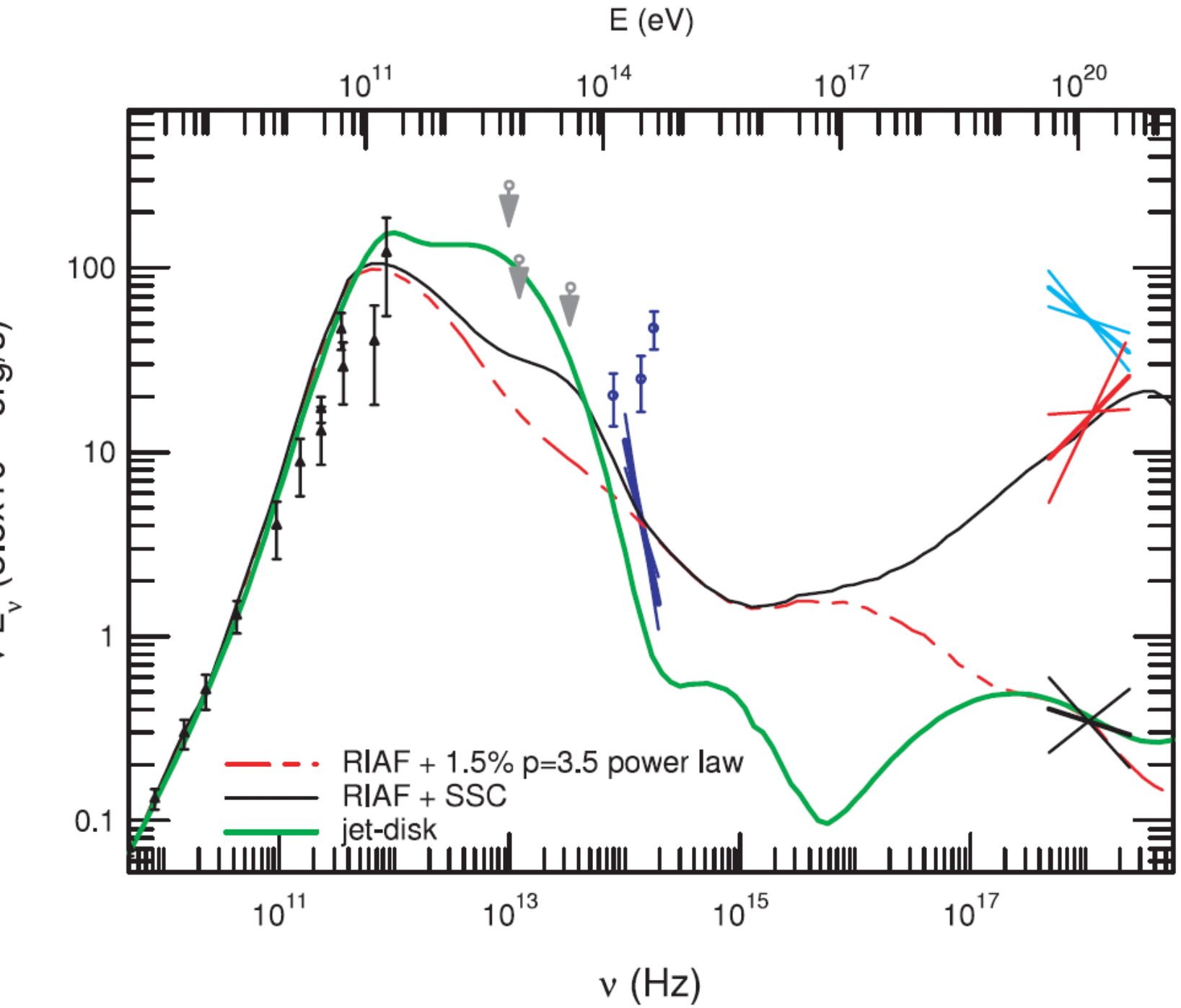

SgrA* & the extended source G2

G2 was supposed a cloud of cold gas with a close (150 AU)encounter with SgrA* in 2014, implying a long lasting X-ray and radio flare. *Schartmann + 2012: simulation*

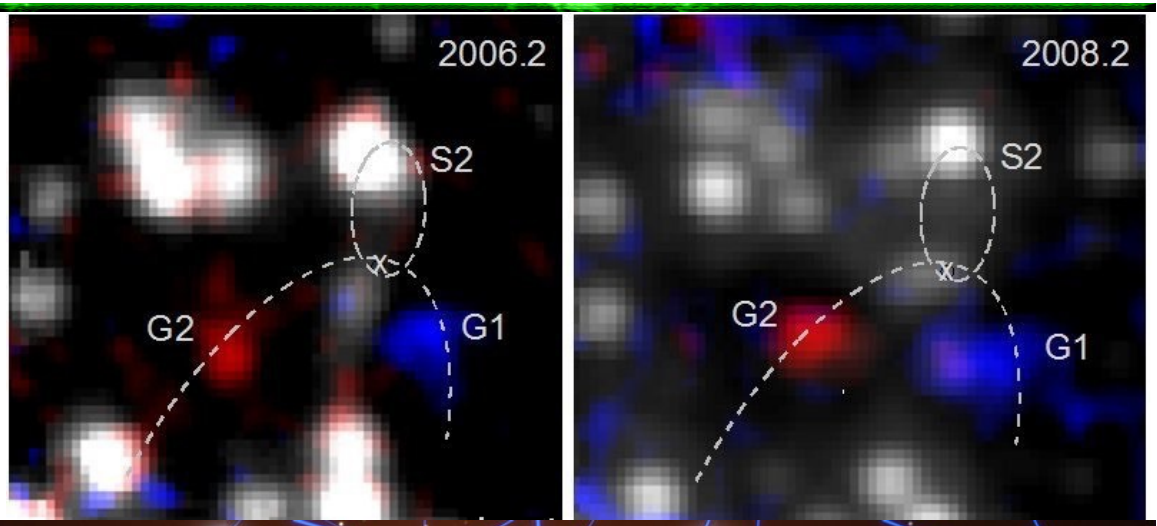

No flare, to date!

Likely a perturbed star, Not a cloud

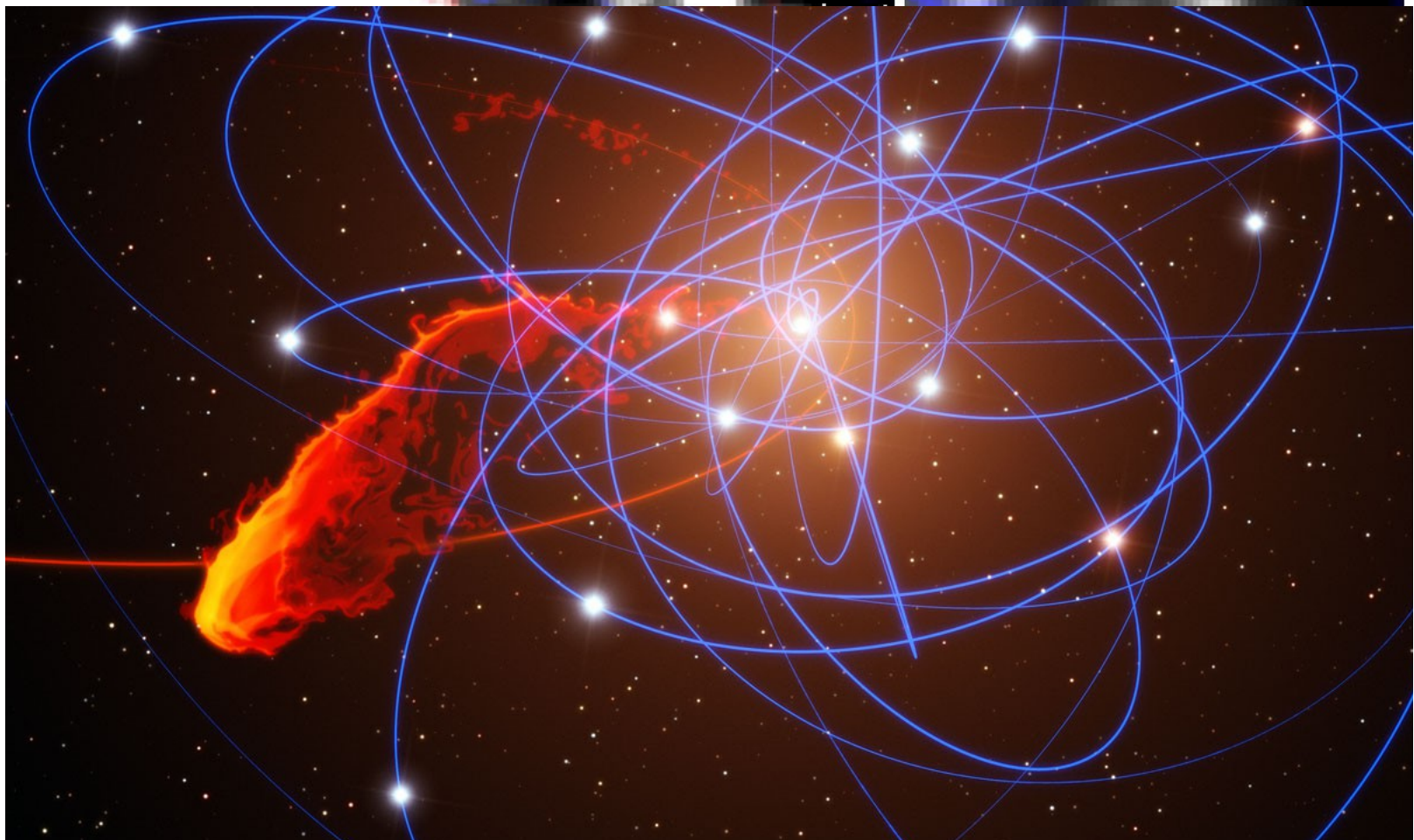

Summary:

https://www.youtube.com/watch?v=xyjqHRNtEto

Unexpectedly, evidence of substantial active star formation within a few pc from SgrA*:

Molecular gas, HII regions, SNR, 100s of O(B) stars

Measure of the mass of the BH : ~ 4 x 106 Msun

X – ray variability consistent with accretion flow to SgrA*, dominated by relatively small events

Summary:

https://www.youtube.com/watch?v=xyjqHRNtEto

A weak "core" is often found in all (spiral galaxies) galaxies.

Anomalies:

Cold gas

SNR

Massive stars

Astronomers did not begin to figure out where the center was hiding until the early 20th century. Harlow Shapley made a pretty good deduction of its general location by looking at the way star clusters in the rest of the Galaxy were distributed. He concluded it was towards the constellation of Sagittarius, but it took a revolution in infrared telescopes before we finally could precisely see the region.

Morris had predicted a decade ago that a process called dynamical friction would cause stellar black holes to sink toward the center of the Galaxy. Black holes are formed as remnants of the explosions of massive stars and have masses of about 10 suns. As black holes orbit the center of the Galaxy at a distance of several light years, they pull on surrounding stars, which pull back on the black holes. The net effect is that black holes spiral inward, and the low-mass stars move out. From the estimated number of stars and black holes in the Galactic Center region, dynamical friction is expected to produce a dense swarm of 20,000 black holes within three light years of Sgr A*. A similar effect is at work for neutron stars, but to a lesser extent because they have a